

Inference for travel time on transportation networks

Mohamad Elmasri^{1*}, Aurélie Labbe², Denis Larocque² and Laurent Charlin²

¹Department of Statistical Sciences, University of Toronto

²Department of Decision Sciences, HEC Montréal

Abstract

Travel time is essential for making travel decisions in real-world transportation networks. Understanding its distribution can resolve many fundamental problems in transportation. Empirically, single-edge travel-time is well studied, but how to aggregate such information over many edges to arrive at the distribution of travel time over a route is still daunting. A range of statistical tools have been developed for network analysis; tools to study statistical behaviors of processes on dynamical networks are still lacking. This paper develops a novel statistical perspective to specific type of mixing ergodic processes (travel time), that mimic the behavior of travel time on real-world networks. Under general conditions on the single-edge speed (resistance) distribution, we show that travel time, normalized by distance, follows a Gaussian distribution with universal mean and variance parameters. We propose efficient inference methods for such parameters, and consequently asymptotic universal confidence and prediction intervals of travel time. We further develop path(route)-specific parameters that enable tighter Gaussian-based prediction intervals. We illustrate our methods with a real-world case study using mobile GPS data, where we show that the route-specific and universal intervals both achieve the 95% theoretical coverage levels. Moreover, the route-specific prediction intervals result in tighter bounds that outperform competing models.

Keywords: Central limit theorem, Mixing sequences, Prediction intervals, Processes on dynamic networks, Travel time estimation.

*Main and corresponding author (mohamad.elmasri@utoronto.ca). ME gratefully acknowledge the funding of *NSERC PDF*; major part of this work was conducted at the Department of Decision Sciences, HEC Montréal and Mila - Quebec Artificial Intelligence Institute.

1 Introduction

Urban mobility is increasingly vital for city planning. Growing population as well as new modalities and systems of transportation are challenging for our current transportation networks. Governments are adopting smart transportation initiatives, such as autonomous and on-demand public transportation (Salazar et al., 2018). Large-scale trip-level data with both temporal and spatial coverage—for example based on global positioning systems (GPS) data from mobile phones or collected from fixed traffic monitoring cameras or other sensors such as Bluetooth and/or WiFi—may enable us to better diagnose current problems and develop solutions to these congestion problems.

At the heart of many of these developments is the estimation of travel-time between locations. Online routing services and ride-share providers,¹ with millions of daily requests, make all those operational and pricing decisions based on estimates of travel time.² These complex decision-making processes require, first, a good understanding of the distribution of travel time, and second, robust inference methods for various quantities of this distribution.

A *route* ρ on a transportation network G consists of an n -sequence of connected edges $\rho = \langle e_1, e_2, \dots, e_n \rangle$ that define the order of travel. Travel time \mathcal{T}_ρ is then defined as a random variable through the partial sum

$$\mathcal{T}_\rho := \sum_{e \in \rho} d_e S_e, \quad (1)$$

where $1/S_e$ is the average speed over the edge e of unit length d_e .

Access to the distribution of \mathcal{T}_ρ may allow the development of a new class of statistical approaches for transportation problems. Here are two examples. First, accounting for uncertainty in route recommendation—especially for emergency medical services—can require testing the hypothesis that travel time on route ρ is faster or less variable than on an alternative route ρ' ,

$$H_1 : \mathbb{E}[\mathcal{T}_\rho] < \mathbb{E}[\mathcal{T}_{\rho'}] \text{ and/or } \mathbb{V}[\mathcal{T}_\rho] < \mathbb{V}[\mathcal{T}_{\rho'}].$$

Second, trip-specific prediction intervals of travel time can be crucial in assessing pricing variability for ride-share providers, enabling a better control on risk.

The distribution of speed S_e in (1) is well-studied empirically. Travel time on each edge as well as the total travel time appears to be log-normally distributed (Gao et al., 2009; Lo, 2012). Yet, the log-normal, unlike the normal, is not a stable distribution, meaning that any linear combinations of it is not necessarily log-normally distributed. Hence, aggregating information on edges to obtain a distribution for \mathcal{T}_ρ , through the partial sum in (1),

¹As examples, Google Maps (maps.google.com), Lyft Inc., and Uber Inc.

²www.forbes.com/.../uber-says-its-doing-1-million-rides-per-day-140-million-in-last-year

is still daunting. Researchers have proposed different methods to estimate travel-time distribution, for example by factoring-out path uncertainty (Hunter et al., 2009; Jenelius and Koutsopoulos, 2013; Zheng and J van Zuylen, 2013), by jointly modeling travel time and the path taken (Wang et al., 2019; Westgate et al., 2013), or by using log-normal mixtures to capture congestion patterns (Guo et al., 2012; Woodard et al., 2017).

On one hand, the statistics community has shown a marked interest in developing tools for network analysis, and good references exist Kolaczyk (2009); Kolaczyk and Csárdi (2014). On the other hand, there is a large amount of work to model processes on network graphs Barrat et al. (2008), with applications in neuroscience, epidemiology and engineering. However, most of this work is of a mathematical nature, and statistical work on such problems is limited with some notable exceptions. For example, on forecasting within nonlinear systems by Ramsay et al. (2007), on social network analysis by Britton and O’Neill (2002); Burk et al. (2007); Getoor et al. (2001); Snijders et al. (2017), and on biochemical networks by Golightly and Wilkinson (2005). For a survey on statistical modeling of dynamic epidemiological networks, see Keeling and Eames (2005), and on transportation, see Barrat et al. (2008, ch. 11).

We find that one of the main hurdles facing further statistical development for processes on networks is the lack of a unified field encapsulating such work, which is related to the lack of sufficient high quality time-index network data, to make sensible statistical inferences. Our paper not only model travel time on real-world networks, but also proposes novel statistical inference and prediction methods which could be use to model similar processes on dynamical networks. We adopt some of the transportation lexicon to increase accessibility to a wider audience.

We first attempt to construct travel time as a well-defined stochastic process on certain types of dynamical networks (systems) that we refer to as transportation networks. We characterize the transportation network G as a directed graph with stochastic edge-speed (resistance), by means of integrating important properties of real-world travel time (Section 2).

Under mild regularity conditions, Section 3 shows that without assuming a distribution for speed, \mathcal{T}_ρ can be normalized to a standard normal distribution. Oppenlander (1976) was the first to suggest such a possibility in real-world transportation networks, yet the problem remained open until now. If the distribution of speed over edges is cyclical with respect to time, with repeating patterns, then we show that:

$$n^{-1/2}(\mathcal{T}_\rho - n\mu) \xrightarrow{d} N(0, \sigma^2),$$

for some universal constants (μ, σ) , where \xrightarrow{d} implies convergence in distribution. Without the cyclicity of speed, the results hold for some constants $(\mu(t_0, \rho), \sigma(t_0, \rho))$ representing

the average travel time and its variance, both depending on a starting time initial condition t_0 and route ρ (Section 3.1). Our proofs are established by means of Birkhoff-Khinchin Ergodic theorem, recurrence propriety of planar graphs, and some recent developments in probabilistic dynamical systems (Limic et al., 2018).

No trip travels for ever, even so, our results enable efficient estimates $(\hat{\mu}, \hat{\sigma})$ of the universal constants (μ, σ) from representative sample trips from the network G . Given m representative sample trips, for a $\beta \in (0, 1)$, a point-wise asymptotic $(1 - \beta)100\%$ prediction interval for a new trip $\mathcal{T}_\rho^{\text{new}}$ over an arbitrary route ρ of n edges is

$$n^{-1}\mathcal{T}_\rho^{\text{new}} \in \left[\hat{\mu} - T_{\beta/2}^{(m-1)} \sqrt{\frac{\hat{\sigma}^2}{n} \left(1 + \frac{1}{m}\right)}, \quad \hat{\mu} + T_{1-\beta/2}^{(m-1)} \sqrt{\frac{\hat{\sigma}^2}{n} \left(1 + \frac{1}{m}\right)} \right],$$

where $T_\beta^{(m)}$ is the β -quantile of the student-t distribution with m degrees of freedom. More details are available in Sections 3.4 and 3.5.

We study prediction intervals for single trips in Section 4, where we propose trip-specific parameters that enable more tailored and tighter intervals. We report the results of real-world case study using GPS data collected from mobile phones in Quebec City in Section 5 and show that our proposed approach compares favourably to previous empirical approaches for travel-time estimation.

2 Travel time as a random variable

This paper takes a constructive approach to travel time defined in (1) by focusing on understanding its distribution on a specific route ρ . The main difficulty in inferring the distribution of \mathcal{T}_ρ , in the real-world, is the different sources of dependencies affecting the distribution of speed $(S_e, e \in \rho)$, which we summarize in three categories:

within-trip (serial) dependency refers to the dependency between speed on consecutive edges within the same trip (a trip view);

across-trip (distributional) dependency refers to the dependency of speed across distinct trips driving the same route and starting (approximately) at the same time (map view); and

filtration (time) dependency refers to the fact that, from a trip view, the distribution (choice) of speed at an edge depends on the arrival time at that edge, and hence on the travel time up to that edge.

Filtration and within-trip dependency arise from different sources. Filtration dependency arise from the dependency of speed distribution on time, which is caused from various

congestion patterns in the real-world. Although the distribution of speed on an edge (map view) can safely be approximated by a mixture distribution (Norets, 2010), only a limited set of mixture components are available at any given time. In the real-world for example, at night, it is safe to assume that all roads are fairly empty, and conditional on that, one can ignore the filtration dependency for trips conducted within those times, since the distribution of speed, i.e. the mixture weights, are fixed for a large time period. On the other hand, filtration dependency is strongest around rush hours. A trip starting right before a rush hour might encounter rush-hour congestion at some edges in the route, those edges are not known at the start of the trip.

Within-trip dependency stems from vehicle behavior, and is structurally different from filtration. It is strongest on non-congested highways. For example, a driver that tends to drive faster than average speed can sustain such behavior longer on highways, especially when non-congested. Congestion and network topology both have a causal effect on within-trip dependency.

Across-trip dependency, although known to be marginal in most cases, is important in characterizing the joint distribution of travel time for multiple trips. Since our focus is on the distribution of travel time for single trips, we will assume no, or negligible, across-trip dependency.

Understanding the sources of dependency in travel time can provide a clearer picture of the behavior of the partial sum in (1). Within-trip dependency is injected by the driver via the selection process of speed at each edge. Filtration and across-trip dependency are induced by factors, such as congestion and network topology, that affect the range and distribution of available speeds a driver can choose from at a specific time. Such dynamics suggest that travel time is a sampling process over a dynamical network G .

2.1 Transportation networks

We define a transportation network $G = (N, E, D, S)$ as a directed connected graph (N, E, D) consisting of a finite *node* set N and an *edge* set E . For each edge $e \in E$, $d_e \in D$ defines the edge traversal positive distance, and $S_e \in S$ defines a set of positive random variables representing the reciprocal of speed. Consequently, $(d_e S_e(t), e \in E)$ represents the travel time of edge e at time $t > 0$, whenever S_e is parameterized by t . G is connected in the sense that there exist a traversable route between any two nodes of G . A *route* ρ in G consists of an n -sequence of connected edges $\rho = \langle e_1, e_2, \dots, e_n \rangle$ that define the order of travel. We distinguish a route ρ in G by the angle bracket $\langle \cdot \rangle$, such that $\langle e, e' \rangle \in \rho$ is a subroute composed of a pair of edges e and e' . We use $n = \#\{e : e \in \rho\}$ to define the length (number of edges) of ρ . Without loss of generality, we assume that the endpoints of ρ are traveled in full. In practice, the actual traveled distance can be used instead, alongside the

proper conditioning of speed.

From (1), travel time is a weighted sum over conditional speed. By conditioning, we refer to route and historical conditioning. Route-conditioning refers to the fact that the distribution of travel time depends on the type of subsequent (possibly previous) edge. Historical conditioning refers to the conditioning on the trip's history. $S_e(t)$ represents the unconditional distribution of speed on an edge, as in the map view. To distinguish the conditional and the unconditional version of speed, we pair the notation " $e \in \rho$ " with a random variable to refer to the conditional version, as opposed to the notation " $e \in E$ ", which is the unconditional version of speed.

In real-world transportation networks $(S_e, e \in E)$ is a strictly positive and bounded random variable, since it cannot be zero over an edge with positive length. Hence, we define S_e under the following assumptions.

Assumption 1. *Let $t \in \mathbb{R}_{>0}$ be the time index. Suppose that the distribution of speed $S_e(t)$ over an arbitrary edge $e \in E$ has a functional average $m_e(t)$ and a non-stationary variance, such that*

$$S_e(t) := m_e(t) + \epsilon_e(t), \quad (2)$$

where

- (i) for all $t > 0$, $S_e(t) \in \mathcal{C}_e = [\delta_e, M_e]$ for some $0 < \delta_e < M_e < \infty$;
- (ii) $m_e(t) := \mathbb{E}[S_e(t)]$ is continuous with respect to t ; and
- (iii) $\mathbb{E}[\epsilon_e(t)] = 0$ with $\sigma_e^2(t) := \mathbb{E}[\epsilon_e^2(t)] > 0$ is continuous with respect to t .

Stationarity of $\sigma_e(t)$ is practically unnecessary since speed is bounded. On the other hand, the periodic empirical behavior of $m_e(t)$ is well studied and shown in the literature in different forms, using temporal decomposition of speed data (Jenelius and Koutsopoulos, 2013; Wang et al., 2019; Woodard et al., 2017; Zheng and J van Zuylen, 2013). It is possible that there exists multiple periodic trends, in the real-world, for the same edge e , which can be modeled additively through the functional mean $m_e(t)$.

Empirically, the periodicity of $(m_e(t), e \in E)$ is not universal (i.e., seasonal), it can be temporary and can shift with time. Periodicity of speed on edges are also timely coordinated over large areas of real-world networks. One example is morning (evening) rush hours. We refer to such timely and wide-spread patterns as *speed regimes*, and define them as follows.

Assumption 2. *There exist a random variable Π representing the speed regimes, such that $m_e(t) \perp\!\!\!\perp m_{e'}(t) \mid \Pi$ for distinct edges $e, e' \in E$, for all times $t \in \mathbb{R}_{>0}$.*

With sufficient data, speed regimes and switching time between them, can easily be captured in a spatio-temporal decomposition. Assumptions 1 and 2 attempt to capture the dynamics of real-world transportation networks using a general framework. The next section formalizes travel time as sampling process.

2.2 Travel time as a sampling process

From a trip view, $(S_e, e \in \rho)$ are sequential samples from edges in ρ over the transportation network G . For a given route, $\rho = \langle e_1, e_2, \dots, e_n \rangle$, the sampling occurs at the random entrance times $\tau(e_1) < \tau(e_2) < \dots < \tau(e_n)$, such that $(S_e(\tau), e \in \rho) = (S_{e_1}(\tau(e_1)), S_{e_2}(\tau(e_2)), \dots)$. The random entrance times can be defined by a sequence of stopping-times $(\tau(e), e \in \rho)$ as

$$\tau(e) := \min\{t > 0 : \mathcal{T}_{\langle \dots, e \rangle} \leq t\}, \quad (3)$$

where $\langle \dots, e \rangle$ is the route up to edge e . From (2), travel time is constructed as

$$\mathcal{T}_\rho := \sum_{e \in \rho} d_e S_e(\tau) = \sum_{e \in \rho} d_e m_e(\tau) + \sum_{e \in \rho} d_e \epsilon_e(\tau). \quad (4)$$

We removed the indexing of τ since it is already implied by the subscript of the functional. From Assumption 1, the residual $(\epsilon_e(\tau), e \in \rho)$ are not identically distributed. They are also dependent as a result of within trip dependency. Finally, $(S_e, e \in \rho)$ is non-stationary, since stationarity implies that all edges must have the same variance and unit distance, both are empirically invalid in real-world transportation networks.

Travel time is empirical in nature and the joint distribution $\mathbb{P}(S_e, e \in \rho)$ is not tractable. Dependency of random variables cannot be measured without knowing the true generating distribution. Nonetheless, it is widely accepted, and empirically shown in many studies, that conditional on a speed regimes, across-trip dependency is low, and within-trip dependency decreases with distance; see for example (Woodard et al., 2017, Figure 5). This form of dependency, which states that random variables far apart are nearly independent, is coined by the seminal paper Rosenblatt (1956) that introduces the “ α -mixing” coefficient to measure such dependency.

Definition 2.1. Let $(X_k, k \in \mathbb{Z})$ be a sequence of random variables defined on the probability space (Ω, \mathcal{F}, P) . Define the σ -algebra \mathcal{F}_a^b as $\mathcal{F}_a^b := \sigma(X_k, a \leq k \leq b, k \in \mathbb{Z})$, $1 \leq a \leq b \leq \infty$. For each $n \geq 1$ define the measure of dependence

$$\alpha(n) := \sup_{k \geq 1} \sup_{A \in \mathcal{F}_1^k, B \in \mathcal{F}_{k+n}^\infty} |P(A \cap B) - P(A)P(B)|. \quad (5)$$

If $\alpha(n) \rightarrow 0$ as $n \rightarrow \infty$, then $(X_k, k \in \mathbb{Z})$ is said to be α -mixing (strongly mixing).

Many results for sequences of independent random variables can be established for strongly mixing sequences. Another measure of dependence, the ρ^* -mixing coefficient, exists and is defined below.

Definition 2.2. Following 2.1, let $(X_k, k = 1, \dots, n)$, and $\mathcal{F}_I = \sigma(X_i, i \in I)$ for any non-empty set $I \subset \{1, \dots, n\}$. Define the dependency measure

$$\rho^*(n) := \sup_{A, B, \text{dist}(A, B) \geq n} \sup_{f, g} |\text{Corr}(f, g)|, \quad f \in \mathcal{L}^2(\mathcal{F}_A), g \in \mathcal{L}^2(\mathcal{F}_B) \quad (6)$$

where $\mathcal{L}^2(\mathcal{F})$ denotes the space of square-integrable \mathcal{F} random variables, where the sup is over all sets that differ by at least n elements.

The coefficient $\rho^*(n)$ is related to the *maximal correlation inequality*, although we define it here for sets that are at least n elements apart $\text{dist}(A, B) > n$. The objective of Definition 2.2 is to insure that there is no disjoint sets of random variables that are fully correlated. Refer to Bradley (2005) for a concise survey on dependent random variable.

Motivated by Definitions 2.1 and 2.2, we assume that the sequence $(S_e, e \in \rho)$ is α -mixing with $\rho^*(1) < 1$, and define travel time as follows.

Definition 2.3 (Travel time random variable). For a transportation network G and a start time t_0 , the travel time \mathcal{T}_ρ in (4) is a random variable constructed by a non-stationary α -mixing sampling over an arbitrary route ρ at the random times $(\tau(e), e \in \rho)$ defined in (3) from processes $(S_e, e \in E)$, with $\rho^*(1) < 1$.

With this construction, we motivate the study of travel time through a visual example. Figure 1 illustrates a toy example of two vehicles traveling on the same 100-edges route, and starting at a similar time. The travel time up to edge e , is clearly different for each vehicle. Yet this does not imply that the long term travel behavior of the two vehicles is different, as shown at $e = 100$. The short-run difference can be the cause of various traffic events. Some of those events are random (unanticipated), others are deterministic, for example traffic lights. Not all deterministic events require conditioning (modeling), since many such events become noise in the long run (one example is traffic lights). This brings us to the study of long-term behavior of travel time via the theory of averaging.

3 Asymptotic properties of travel time

Estimating long-term behavior of the travel time defined in 2.3 requires treatment of the last form of dependency, which is the dependency on the random times $(\tau_e, e \in \rho)$ in (4). We refer to such dependency as *filtration* rather than time (or entrance time) dependency, since

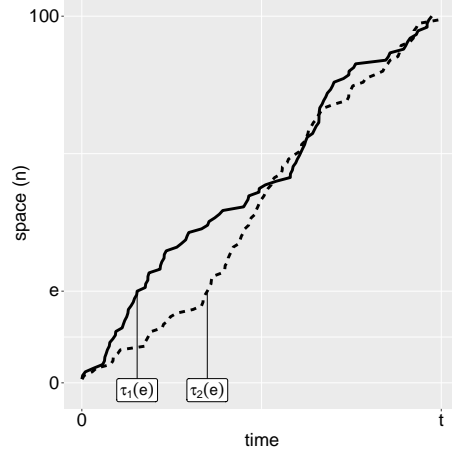


Figure 1: A toy example of two vehicles traveling a 100-edge route, starting at the same time, with $\tau_i(e), i = 1, 2$, being the vehicles random arrival times at e .

the distribution of speed over an edge e at a future time t is measurable (by assumption 1, S_e is bounded and continuous), and hence can be approximated by a Gaussian mixture (Ghosh et al., 2003; Nestoridis et al., 2011; Norets, 2010)). The variability of such measurement can be large, and precise information on the distribution of speed over an edge at future time t , depends on all information up (or very close) to time t . Such information includes, though is not restricted to, environmental variables and other finite shock events to the system, accidents as an example.

We treat such dependency in two ways that we call *online* and *offline* (stationary) systems. The online system assumes that the average speeds $(m_e(t), e \in \rho)$ vary randomly with respect to time, and hence cannot be modeled from data. This system does not represent the realities of real-world transportation networks, nonetheless, we show that a central limit (CLT) representation is possible with asymptotic parameters that depend on the starting time of the trip (i.e. initial conditions). The offline system supposes the seasonality of $(m_e(t), e \in \rho)$ with respect to time with repetitive periodic patterns. This system is closer to the realities of the real-world. As a result, sequences of expectations and variances converge asymptotically to universal constants (μ, σ^2) that are independent of initial conditions. This allows a universal CLT representation.

Let (Ω, \mathcal{F}, P) be a probability space over a transportation network G , where \mathcal{F} is the natural filtration as $\sigma(S_e(t), t > 0, e \in E)$, and $(\mathcal{F}_t, t > 0)$ is the continuous-time filtration with real time index $t > 0$, defined on the whole network as the σ -algebra $\mathcal{F}_t = \sigma(S_e(s), s < t, e \in E)$. By the continuity of $(m_e(t), e \in E)$, $(S_e(t), e \in E)$ and \mathcal{T}_ρ are \mathcal{F}_t -measurable for

all time $t \geq 0$. In addition, \mathcal{T}_ρ is also measurable with respect to its own stopping time filtration $(\mathcal{F}_{\tau(e)}, e \in \rho)$, where $(\tau(e), e \in \rho)$ is defined in (3), see [Kallenberg \(2006, Lem 6.5\)](#). The expected value of \mathcal{T}_ρ , $\mu_\rho(\tau)$, is constructed by conditioning on its own stopping-time $(\mathcal{F}_{\tau(e)}, e \in \rho)$, as

$$\mu_\rho(\tau) := \sum_{e \in \rho} d_e \mathbb{E}[S_e(\tau) \mid \mathcal{F}_{\tau(e)}] = \sum_{e \in \rho} d_e m_e(\tau) + \sum_{e \in \rho} d_e \mathbb{E}[\epsilon_e(\tau) \mid \mathcal{F}_{\tau(e)}]. \quad (7)$$

The exact value of $m_e(\tau)$ in (7) is only known at time $\tau(e)$. Hence, $\mu_\rho(\tau)$ is an online mean, updated at each edge $e \in \rho$. Similarly, the online variance is

$$\sigma_\rho^2(\tau) := \sum_{e \in \rho} d_e^2 \sigma_e^2(\tau) + \sum_{e, e' \in \rho} d_e d_{e'} \mathbb{V}(\epsilon_e(\tau), \epsilon_{e'}(\tau) \mid \mathcal{F}_{\tau_{\max}}) \quad (8)$$

where $\tau_{\max} = \max\{\tau(e), \tau(e')\}$, $\sigma_e^2(\tau) := \mathbb{E}[\epsilon_e^2(\tau) \mid \mathcal{F}_{\tau(e)}] - \mathbb{E}[\epsilon_e(\tau) \mid \mathcal{F}_{\tau(e)}]^2$. Under the online system, the online mean in (7) and variance in (8) converge to constants that depends on initial conditions, shown in the next section. Under the offline system, they converge to universal constants.

3.1 Online system

With (7) and (8), we derive a point-wise strong law of large numbers for travel time, with proofs in [Appendix A](#).

Lemma 3.1. *Let ρ be an increasing route on a transportation network G . With a starting time t_0 (i.e., initial conditions), let \mathcal{T}_ρ be as defined in [2.3](#), then $n^{-1}\mathcal{T}_\rho \xrightarrow{n} \mu(t_0, \rho)$ almost surely (a.s.), where $\mu(t_0, \rho)$ is a constant that depends on initial conditions t_0 and route ρ .*

The proof in [Appendix A](#) relies on the fact that speed is bounded and $\rho^*(1) < 1$ from [Definition 2.3](#). Alternative methods exist for strong convergence, for example, if $\sum_{n=1}^{\infty} n^{-1}\alpha(n) < \infty$, see [Volkonskii and Rozanov \(1959, Lem 1.1\)](#) and [Berbee \(1987, Thm 1.2\)](#). For convergence in probability (weak law of large numbers), $\alpha(n) \rightarrow 0$ is sufficient by the Markov inequality.

Despite the limiting result of [Lemma 3.1](#), that $\mu(t_0, \rho)$ is not estimable at the start of the trip; motivated by [Peligrad \(1996\)](#), we introduce a central limit theorem for travel time, with proof in [Appendix B](#).

Theorem 3.2 (CLT for travel time). *Let \mathcal{T}_ρ be as defined in [2.3](#). Let $\mu_\rho(\tau)$ and $\sigma_\rho^2(\tau)$ be as defined in (7), (8), respectively. For any initial condition t_0 , $n^{-1}\sigma_\rho^2(\tau) \rightarrow \sigma^2(t_0, \rho)$ a constant. If $\sigma^2(t_0, \rho) \neq 0$, then*

$$n^{-1/2}(\mathcal{T}_\rho - n\mu(t_0, \rho)) \xrightarrow{d} N(0, \sigma^2(t_0, \rho)) \quad \text{as } n \rightarrow \infty.$$

The pair of constants $(\mu(t_0, \rho), \sigma^2(t_0, \rho))$ both depend on the initial condition t_0 and the route ρ . The proof follows from known results on α -mixing sequences, convergence rates are also accessible from literature, although with extra conditions on the mixing rate $\alpha(n)$.

Without extra conditions on G , Theorem 3.2 suggests that i) even though, the increments $\Delta\mathcal{T}_\rho = \mathcal{T}_{\langle \dots, e', e \rangle} - \mathcal{T}_{\langle \dots, e' \rangle}$ are not independent, nor identically distributed, they are well-behaving enough; and ii) each trip is normally distributed given its own mean and variance. The next section imposes extra conditions on G that allow for stronger results, a trip-invariant central limit theorem, with universal parameters (μ, σ) .

3.2 Offline (stationary) system

To strengthen the results of Lemma 3.1, we define G to be a stationary transportation network if $(m_e(t), e \in E)$ in (2) is seasonal, leading to Theorem 3.3.

Theorem 3.3. *Let ρ be a random walk on a stationary transportation network G . Let \mathcal{T}_ρ be as defined in 2.3, then*

$$\frac{\mathcal{T}_\rho}{n} \xrightarrow{n} \mu, \quad \text{a.s.}, \quad (9)$$

where μ is the invariant expected speed defined as $\mu = \sum_{e \in E} \pi_e \mu_e$, with $\mu_e = d_e \mathbb{E}[S_e]$ the unconditional average travel time over e and π_e is the stationary probability of traveling e .

Sketch proof. We treat the residual part of the sum in (4) through its α -mixing property. By the recurrence property of random walks on finite graphs, Birkhoff's ergodic theorem, and some recent advances in probabilistic dynamical systems (Limic et al., 2018), we show that the sum $n^{-1} \sum_{e \in \rho} d_e m_e(\tau)$ is ergodic, hence converges to a constant μ that is independent of initial conditions. See Appendix C for a full proof. \square

Because travel time is an empirical process, we built on the fact that ρ is a random walk in G , in Theorem 3.3. Many deterministic systems are essentially random walks in the limit, see the examples given by Aldous (1991). If ρ is cyclical, the results still hold, since the subgraph constructed from the cycle is still a transportation network, and μ would depend on it. We now establish a stronger CLT, with proof in Appendix B.

Theorem 3.4 (CLT for travel time on stationary networks). *With the notations in 3.2, let G be a stationary transportation network, with ρ being a random walk on G , and let μ be as in (9). Then, $n^{-1} \sigma_\rho^2(\tau) \rightarrow \sigma^2$, a constant. If $\sigma^2 \neq 0$, then*

$$n^{-1/2}(\mathcal{T}_\rho - n\mu) \xrightarrow{d} N(0, \sigma^2) \quad \text{as } n \rightarrow \infty. \quad (10)$$

Both μ and σ^2 are independent from initial condition and ρ .

The highlight of Theorem 3.4 is that independently of the start time and route, the longer one drives the closer its average is to a single universal constant μ , with universal standard deviation σ . The condition that $\sigma^2 \neq 0$ is not as stringent in real-world transportation networks, since speed limits vary across edges.

The online system, Theorem 3.3 in particular, suggest that $\mu(t_0, \rho)$ might differ for different initial conditions t_0 . The topology of real-world transportation networks is fixed, and speed is bounded. The only reason one would expect wide differences for different initial conditions is if traffic flow of the network dramatically changed over time with no periodicity. This is not the case in practice; the gap between the online and offline systems could be marginal. Hence, we focus on estimating the parameters of the latter.

3.3 Estimation of (μ, σ)

By ergodicity of the offline system, the expected value of the average travel time over an arbitrary route of length n is μ , as $\mathbb{E}[n^{-1}\mathcal{T}_\rho|n] = \mu$, for all $n \in \mathbb{Z}$. This expectation is with respect to the stationary distribution $(\pi_e, e \in E)$. By treating n as a random variable, by law of total variance, the unconditional variance of average travel-time is

$$\begin{aligned}\mathbb{V}(n^{-1}\mathcal{T}_\rho) &= \mathbb{E}[\mathbb{V}(n^{-1}\mathcal{T}_\rho | n)] + \mathbb{V}(\mathbb{E}[n^{-1}\mathcal{T}_\rho | n]) = \mathbb{E}[n^{-1}(\sigma^2 + O(n))] + \mathbb{V}(\mu) \\ &= \sigma^2\mathbb{E}[n^{-1}]\end{aligned}\tag{11}$$

With a slight abuse of notation, $O(n)$ represents the residual as a random variable of the average variance of travel time, essentially $n^{-1}\mathbb{V}(\mathcal{T}_\rho) - \sigma^2 = O(n)$. The expectation with respect to distance of $\mathbb{E}[n^{-1}O(n)] = \sum_{n_0} \mathbb{P}(n = n_0)n_0^{-1}\mathbb{E}[O(n_0)] = 0$, since the latter is an expectation with respect to time.

With the above two identities, given a representative independent sample of m trips $\mathcal{T}_\rho^{(j)}$, $j = 1, \dots, m$, with n_j edges each, the M-estimator of μ is

$$\hat{\mu} = \frac{1}{m} \sum_{j=1}^m \frac{\mathcal{T}_\rho^{(j)}}{n_j}.\tag{12}$$

By conditioning on n_j , with the laws of total expectation and variance, $\mathbb{E}[\hat{\mu}]$ and $\mathbb{V}(\hat{\mu})$ can be analytically defined as, $\mathbb{E}[\hat{\mu}] = m^{-1} \sum_{j=1}^m \mathbb{E}[\mathbb{E}[n_j^{-1}\mathcal{T}_\rho^{(j)} | n_j = n]] = \mu$, and

$$\mathbb{V}(\hat{\mu}) = \mathbb{E}[\mathbb{V}(\hat{\mu} | n)] + \mathbb{V}(\mathbb{E}[\hat{\mu} | n]) = \frac{1}{m^2} \sum_{j=1}^m \mathbb{E}\left[\frac{1}{n}[\sigma^2 + O(n)]\right] + \mathbb{V}(\mu) = \frac{\sigma^2}{m}\mathbb{E}[n^{-1}].\tag{13}$$

For a fixed route length, such as $n_j = n$ for all $j = 1, \dots, m$, $\mathbb{V}(\hat{\mu}) = \{mn\}^{-1}\sigma^2$; if $n = 1$ we retrieve the classical sample mean variance $m^{-1}\sigma^2$. Applying the classical CLT on the

convergence of sample mean we have

$$\sqrt{m}(\hat{\mu} - \mu) \xrightarrow{d} N(0, \sigma^2 \mathbb{E}[n^{-1}]), \quad \text{as } m \rightarrow \infty. \quad (14)$$

Since $\hat{\mu}$ is an unbiased estimator of μ , from (11) and $\mathbb{E}[n^{-1}\mathcal{T}_\rho|n] = \mu$, a consistent and unbiased estimator of the unconditional variance $\sigma^2 \mathbb{E}[n^{-1}]$ is

$$\widehat{\mathbb{V}}(n^{-1}\mathcal{T}_\rho) = \frac{1}{m-1} \sum_{j=1}^m (n_j^{-1}\mathcal{T}_\rho^{(j)} - \hat{\mu})^2. \quad (15)$$

The variance³ σ^2 in Theorem 3.4 represents the limit of the conditional variance $n^{-1}\mathbb{V}(\mathcal{T}_\rho|n)$, while $\mathbb{V}(n^{-1}\mathcal{T}_\rho)$ is the total variance that treats n as random quantity.

Let $\widehat{\mathbb{E}}[n^{-1}] = m^{-1} \sum_{j=1}^m n_j^{-1}$, from (15), a profile estimator of σ^2 is

$$\hat{\sigma}_{\text{prof}}^2 = \frac{\widehat{\mathbb{V}}(n^{-1}\mathcal{T}_\rho)}{\widehat{\mathbb{E}}[n^{-1}]}. \quad (16)$$

3.4 Confidence intervals

The normality results for the online and offline systems allow easy construction of confidence intervals for the average travel time μ . For a large sample of m trips, from (14), the classical CLT $(1 - \beta)100\%$, $\beta \in (0, 1)$, confidence interval around μ of the offline system is

$$\mu \in \left[\hat{\mu} - T_{\beta/2}^{(m-1)} \sqrt{\frac{\widehat{\mathbb{V}}(n^{-1}\mathcal{T}_\rho)}{m}}, \quad \hat{\mu} + T_{1-\beta/2}^{(m-1)} \sqrt{\frac{\widehat{\mathbb{V}}(n^{-1}\mathcal{T}_\rho)}{m}} \right], \quad (17)$$

where $\hat{\mu}$ as in (12), and $\widehat{\mathbb{V}}(n^{-1}\mathcal{T}_\rho)$ as in (15), $T_{\beta}^{(m)}$ is the β -quantile of a student-t distribution with m degrees of freedom. For very large m , $T_{\beta}^{(m)} \approx z_{\beta} = \inf\{x \in \mathbb{R} : 1 - \Phi(x) > \beta\}$, where $\Phi(x)$ is the cumulative distribution function of a standard normal random variable.

For the online system, the asymptotic variance can be estimated, for example, by a blocking method (Peligard and Suresh, 1995; Wu, 2009). However, theoretical properties of such estimators are hard to understand because of the lack of stationarity.

³By assuming weak stationarity of the variance), following the argument of Herrndorf (1983, page 99), the variance can be represented as $\sigma^2(n) = nh(n)$, where n is the length of the route, and $h(n)$ is a slow varying function. By Karamata representation theorem for slow varying function, h can be represented as $h(n) = \exp(f(n) + \int_0^n t^{-1}g(t)dt)$, for two bounded measurable functions f and g , where $f(n)$ converges to a constant and $g(n)$ to zero, as $n \rightarrow \infty$. This constitute an alternative approach to modeling the variance.

3.5 Pool-based asymptotic prediction intervals

From (10), we know that $\mathbb{V}(\mathcal{T}_\rho^{\text{new}}) = n\sigma^2$. When the mean and variance are known, the $(1 - \beta)100\%$ intervals of $N(n\mu, n\sigma^2)$ distribution can be used as a prediction interval. When the mean is unknown, and the predictor of $\mathcal{T}_\rho^{\text{new}}$ is $n\hat{\mu}$, and thus, a prediction interval must take into account predictor uncertainty (Geisser, 2017). The route-length conditional variance is $\mathbb{V}(\mathcal{T}_\rho^{\text{new}} - n\hat{\mu}|n) = n\sigma^2(1 + m^{-1})$. Using the profile estimator $\hat{\sigma}_{\text{prof}}^2$ of (16), we have $\hat{\mathbb{V}}(\mathcal{T}_\rho^{\text{new}} - n\hat{\mu}|n) = n\hat{\sigma}_{\text{prof}}^2(1 + m^{-1})$. Based on classical CLT result, a point-wise asymptotic prediction intervals is of the form

$$\mathcal{T}_\rho^{\text{new}} \in \left[n\hat{\mu} - T_{\beta/2}^{(m-1)} \sqrt{n\hat{\sigma}_{\text{prof}}^2(1 + \frac{1}{m})}, \quad n\hat{\mu} + T_{1-\beta/2}^{(m-1)} \sqrt{n\hat{\sigma}_{\text{prof}}^2(1 + \frac{1}{m})} \right]. \quad (18)$$

By conditioning the variance estimate on n , (18) is a pooled interval, in the sense that it will cover with $(1 - \beta)\%100$ level of significance any arbitrary route of length n from the pool of routes of that length. For route (and possibly time) specific (non-pooled) prediction intervals, one would need m independent trip samples of the route (and time) to calculate the parameters $\hat{\mu}, \hat{\sigma}_{\text{prof}}^2$ used in (18).

4 Trip-specific prediction intervals

Most applications are interested in bounding travel time by constructing predictive intervals. Different types of intervals are suitable for different objectives. Network-pooled estimators, as in the universal parameters (μ, σ) of Section 3.3 provide asymptotic bounds in (18) that are wider on the short-term and converges to zero in the long-term. In practice, most trips are short. Hence, the objective of this section is to provide predictive interval sequences that are trip-specific, tighter on the short-term but whose length does not converge to zero in the long-term. Applications in route recommendation for short trips can benefit from such property.

One possible consistent estimate of μ that can capture short-term behaviors is the recursive estimate $\mu_\rho(\tau^*)$, defined at the deterministic mean cumulative travel times $\tau^* = (\tau^*(e), e \in \rho)$. Calculated recursively as $\tau^*(e') = \tau^*(e) + d_e m_e(\tau^*(e))$ for every subroute $\langle \dots, e, e' \rangle \in \rho$, and representing the set of cumulative travel times up to edge e' along the route ρ . Assuming an entrance time t_0 at the first edge, $\mu_\rho(\tau^*)$ is defined as

$$\mu_\rho(\tau^*) := \sum_{e \in \rho} m_e(\tau^*). \quad (19)$$

The cumulative travel times $(\tau^*(e), e \in \rho)$ can also be used to construct a covariance sum similar to the one in (8). This requires the estimation of $2^{-1}n(n + 1)$ terms: n edge \times time

specific variances and $2^{-1}n(n-1)$ pairwise correlation coefficients. This is a daunting task, and a reduced covariance sum that only requires $n+1$ parameters can be used instead, such as

$$\sigma_\rho^2(\tau^*) := \sum_{e \in \rho} d_e^2 \sigma_e^2(\tau^*) + 2\xi_G \sum_{\langle e, e' \rangle \in \rho} d_e d_{e'} \sigma_e(\tau^*) \sigma_{e'}(\tau^*), \quad (20)$$

where ξ_G is a proxy to the average lag-one auto-correlation over G . The sequences $(\mu_\rho(\tau^*), \sigma_\rho^2(\tau^*))$ result in the following asymptotic predictive distribution.

Theorem 4.1 (Predictive distribution of \mathcal{T}_ρ). *With the notations in 3.2 and Assumption 2, let G be a stationary transportation network, with ρ being a random walk on G , and let $\mu_\rho(\tau^*)$ be as in (19) and $\sigma_\rho(\tau^*)$ as in (20), then*

$$\sigma_\rho^{-1}(\tau^*)(\mathcal{T}_\rho - \mu_\rho(\tau^*)) \xrightarrow{d} \sqrt{\eta}N(0, 1 + \tilde{\sigma}^2), \quad (21)$$

where η is a strictly positive constant representing the ratio of $n\sigma^2$ to $\sigma_\rho^2(\tau^*)$, and

$$\tilde{\sigma}^2 = \mathbb{E}[\mathbb{V}(m_e(t)|e)] = \sum_{e \in E} \pi_e \left[\int_{\mathcal{C}_e} m_e^2(t) dt - \left(\int_{\mathcal{C}_e} m_e(t) dt \right)^2 \right].$$

The predictive distributing has more parameters than that of Theorem 3.4, which has two. Yet, the benefit of such method is that i) both $\mu_\rho(\tau^*)$ and $\sigma_\rho(\tau^*)$ are estimable at the start of a trip, since they depend on a recursive argument of deterministic times, and ii) it results in a tighter short-term prediction sequence.

Let $(\{\hat{m}_e, \hat{\sigma}_e^2\}, e \in E)$ be map-version M-estimates of $(\{m_e(\tau^*), \sigma_e(\tau^*)\}, e \in E)$, at times $(\tau^*(e), e \in \rho)$, for a route ρ , define the estimator $\hat{\mu}_\rho(\tau^*)$, of $\mu_\rho(\tau^*)$, as

$$\hat{\mu}_\rho(\tau^*) = \sum_{e \in \rho} \hat{m}_e(\tau^*). \quad (22)$$

Given m representative independent sample of trips $\mathcal{T}_\rho^{(j)}$, $j = 1, \dots, m$, from the system, with route $\rho^{(j)}$ of n_j length each, a pool estimator of ξ_G is

$$\hat{\xi}_G = \frac{1}{m} \sum_{j=1}^m \frac{1}{n_j} \sum_{\langle e, e' \rangle \in \rho^{(j)}} \frac{(S_e^{(j)}(\tau) - \hat{m}_e(\tau))(S_{e'}^{(j)}(\tau) - \hat{m}_{e'}(\tau))}{\hat{\sigma}_e(\tau)\hat{\sigma}_{e'}(\tau)}. \quad (23)$$

$\mathcal{T}_\rho^{(j)}$ are already observed, thus $(\tau(e), e \in \rho^{(j)})$ in (23) are deterministic times, representing the observed entry time in each edge. An estimator of $\sigma_\rho(\tau^*)$ is then.

$$\hat{\sigma}_\rho^2(\tau^*) := \sum_{e \in \rho} d_e^2 \hat{\sigma}_e^2(\tau^*) + 2\hat{\xi}_G \sum_{\langle e, e' \rangle \in \rho} d_e d_{e'} \hat{\sigma}_e(\tau^*) \hat{\sigma}_{e'}(\tau^*), \quad (24)$$

Even though η and $\tilde{\sigma}^2$ are well defined quantities, their estimators can be hard to compute. A classical sample variance estimator can be used for the conditional variance of $\mathbb{V}(m_e(t) | e)$ if large amounts of data per edge at time t is available, otherwise, one requires smoothing or time binning. Therefore we propose a pooled estimator of the total total variance $\nu = \eta(1 + \tilde{\sigma}^2)$ based on the sample variance of the residual of different trips, as

$$\hat{\nu} = \frac{1}{m-1} \sum_{j=1}^m (\varepsilon^{(j)} - \bar{\varepsilon})^2, \quad (25)$$

where $\varepsilon^{(j)} = \{\hat{\sigma}_\rho^{(j)}(\tau^*)\}^{-1}(\mathcal{T}_\rho^{(j)} - \hat{\mu}_\rho^{(j)}(\tau^*))$, and $\bar{\varepsilon} = m^{-1} \sum_{j=1}^m \varepsilon^{(j)}$.

Both $\hat{\nu}$ and $\hat{\xi}_G$ are pooled estimators, not trip specific. By adding higher order covariance terms to the sum in (20), it is possible to reduce the variability resulting from pooling in $\hat{\nu}$. This approach leads to introducing an additional auto-correlation parameter; thus, its utility is application specific.

From Theorem 4.1, the estimators (23) and (25), a $100 \times (1 - \beta)\%$ prediction interval for a new trip is

$$\mathcal{T}_\rho^{\text{new}} \in \left[\hat{\mu}_\rho(\tau^*) - z_{\beta/2} \sqrt{\hat{\nu} \hat{\sigma}_\rho(\tau^*)}, \quad \hat{\mu}_\rho(\tau^*) + z_{1-\beta/2} \sqrt{\hat{\nu} \hat{\sigma}_\rho(\tau^*)} \right], \quad (26)$$

where z_β is the β -quantile of a standard normal.

5 Quebec City case study

We use GPS data collected in 2014 by individuals located in Quebec City (Canada). Our initial Quebec City Data (QCD) contains 21,872 individual trips from over 4,000 drivers. However, no signal is given regarding the validity of each trip; i.e., if they are composed solely from motorized vehicles, excluding walkers, bikers, and non-traffic interruptions. Since our focus is on personal vehicular travel, we partition trips based on recommendations from (Woodard et al., 2017) to remove non-motorized trips, or portions of them. Please refer to Appendix E.1 for the details of this data cleaning process. It is possible that some of the remaining trips are from buses or other transit modes. This is an unavoidable challenge when relying only on mobile phone location data.

Trips are composed of a sequence of GPS readings; the total trip duration is the difference between the first and last GPS timestamps. The final dataset contains 20,554 trips with median and average duration of 19min and 21min, respectively, and a maximum of 3h27min. The median trip distance is 14.5km, mean of 16.6km and maximum of 170.4km. Median and average times between consecutive GPS observations is 4s and 9s, respectively.

We use a third-party service (TrackMatching⁴) to map trips GPS observations to the road network of Quebec City created by The OpenStreetMap Project (OSM);⁵ a publicly accessible open source project. This process is called map-matching. There are numerous high-quality map-matching approaches (Hunter et al., 2013; Newson and Krumm, 2009). For each trip, the third-party service returns a sequence of mapped GPS points with length equal to the original sequence. Each mapped GPS point is associated with a source “node id”, “way id”, and destination “node id”, corresponding to a unique directional edge having “way id” between the source and destination nodes. In rare circumstances, the map-matching service also returns intermediate edges that do not have initial GPS observations; this happens for example when a car is driving very fast or goes through a tunnel. The map-matching process resulted in 46,386 unique directional edges, which constitute the traveled portion of Quebec City, not the entire network. For each trip, total travel time per edge was computed using the method described in Appendix E.1.

Figure 2 shows seasonal (weekly) traffic patterns per hour of week. The volume of traffic is reduced overnight in weekdays starting after 7PM, and during weekends. Daily traffic peaks are associated with AM and PM rush hours, with strong dips in between.

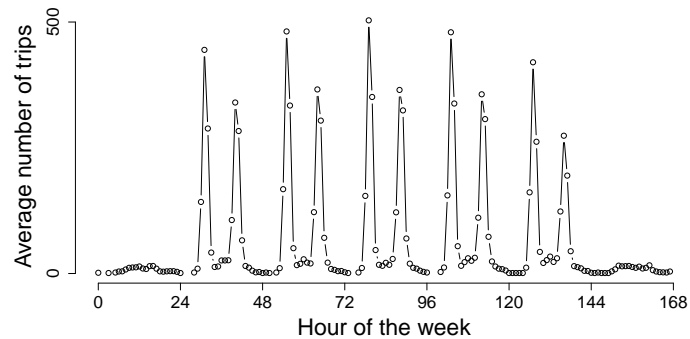


Figure 2: Average number of trips per hour in QCD, by hour of the week.

We start by exploring the data including sampling and time-binning strategies in Section 5.1. Sections 5.2 and 5.3 then evaluate pool-based and trip-specific prediction intervals. We end by comparing the out-of-sample performance of our method against previous proposed methods for travel-time estimation in Section 5.4.

⁴mapmatching.3scale.net

⁵www.openstreetmap.org

5.1 Parameter estimation

Estimating the parameters of Section 3.3 depends on the sampling method of trips. Because of the seasonal traffic pattern illustrated in Figure 2, and the sparsity of GPS data per edge, we compare our results for two sampling methods: i) sampling at random, ii) sampling stratified by three traffic time-bins (traffic-bins). Traffic-bins are discerned from Figure 2, as an i) “AM”-rush-hour bin for weekdays 6:30-8:30AM; a ii) “PM”-rush-hour bin for weekdays 3:30-5PM, and an ii) “Otherwise” bin for all remaining time periods. Alternative time bins have been tested, however, we found that aggregating data in those bins yielded the best results. Note that in QCD, 37% of trips occurred in an AM rush hour, with similar proportion for the PM rush hour, and 26% in all other times. Under the random sampling

Table 1: Parameter estimation under different sampling methods. The “overall” estimate represents the average of the estimate per bin.

	Sampling method				
	At random	Stratified by traffic-bins			
		overall	AM	PM	Otherwise
$\hat{\mu}$	16.70 (16.4,17.1)	16.60 (16.2,16.9)	17.90	17.70	13.70
$\hat{\mathbb{V}}(n^{-1}\mathcal{T}_\rho)$	33.50	34.10	52.90	33.40	23.00
$\hat{\mathbb{E}}[n^{-1}]$	0.02	0.02	0.02	0.02	0.02
$\hat{\sigma}_{\text{prof}}$	41.80	42.20	52.80	39.90	33.00

method, 1000 trips are drawn to calculate the parameters of interest with results reported in Table 1. In parenthesis are the 95% confidence intervals for $\hat{\mu}$, calculated according to (17). For the stratified sampling method, we used 500 trips for each of the substrata (AM, PM, and Otherwise) to estimate the parameters. We classify a trip into a bin if all edges are travelled within that bin (trips overlapping two traffic-bins were removed from the analysis).

To illustrate the empirical ergodicity of the system, Figure 3 reports the space average (dotted lines), for the portion of the first n edges, for each length n , and the time average $\hat{\mu}$ (solid lines), for trips sampled at random (left) and by traffic-bins (right). Space and time averaging are almost exact for both sampling methods, well within the 95% confidence intervals in Table 1. In gray are the progressive averages ($n^{-1}\mathcal{T}_\rho$) of travel time per trip.

5.2 Pool-based asymptotic prediction intervals

To illustrate the asymptotic coverage of our pool-based PI, Figure 4 (left panel) reports the empirical coverage levels (dashed lines) at the theoretical 95% levels for each length n , for 500 test trips, sampled at random. Our pool-based PI of (18), are in solid, with progressive

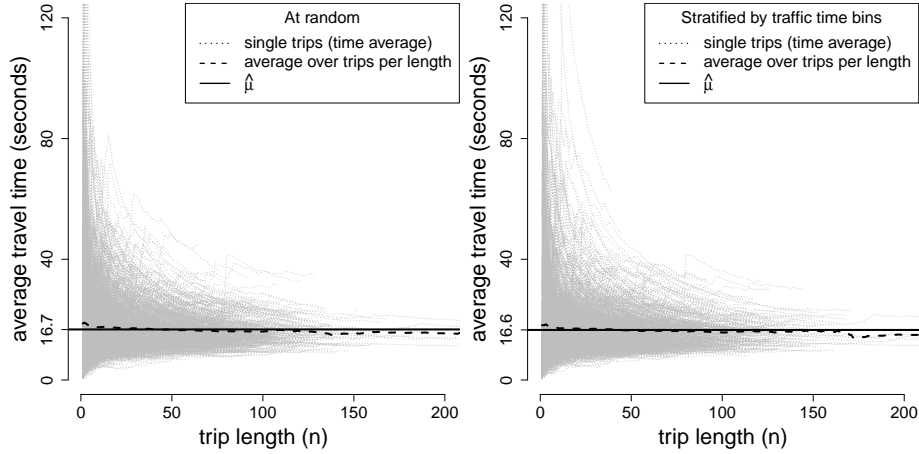


Figure 3: Time and space averaging for 1,000 trips sampled at random (left), and for the 1,500 trips stratified by traffic-bins (overall estimation, right). All trips are of at least 10 edges. Time average of each trip is in gray, dashed lines represent (space) averaging over trips per length, and solid lines are the estimates $\hat{\mu}$.

averages ($n^{-1}\mathcal{T}_\rho$) in gray for each of the 500 trips. The empirical coverage level matches the theoretical 95% level of significance for almost the whole range. Results for different stratas are similar, refer to Appendix Figure 7.

To illustrate the distributional fit, Figure 4 (right panel) reports the histogram of the normalized travel time $(n + nm)^{-1/2}(\mathcal{T}_\rho - n\hat{\mu})$ for the 500 test trips, and the predictive density $\hat{\sigma}_{\text{prof}}T^{(m-1)}$. The value of n is trip specific, while m is the number of samples used for parameter estimation of Table 1. The distributional fit varied between stratas, where the random sampling, PM and Otherwise stratas (Appendix Fig. 7), resulted in better distributional fit than the AM strata, even though the coverage probability is similar. Such discrepancy in fit is the result of i) the asymptotic nature of the PI, and ii) not using route-specific information. The AM strata has many more slower and shorter trips than the sampled at random. By integrating route-specific information, as in our trip-specific prediction sequences (section 5.3), one can correct for such discrepancies.

Table 2 illustrates various numerical results for the same test set used in Figure 4. The average PI length, for a trip sampled at random, is 140.5% of the observed travel time. This number converges to zero theoretically as n increases, as shown in Table 3 that reports model performance under different trip lengths, for the same test set. For trips with $n > 120$, the average PI length drops to 92.2% of the observed travel time.

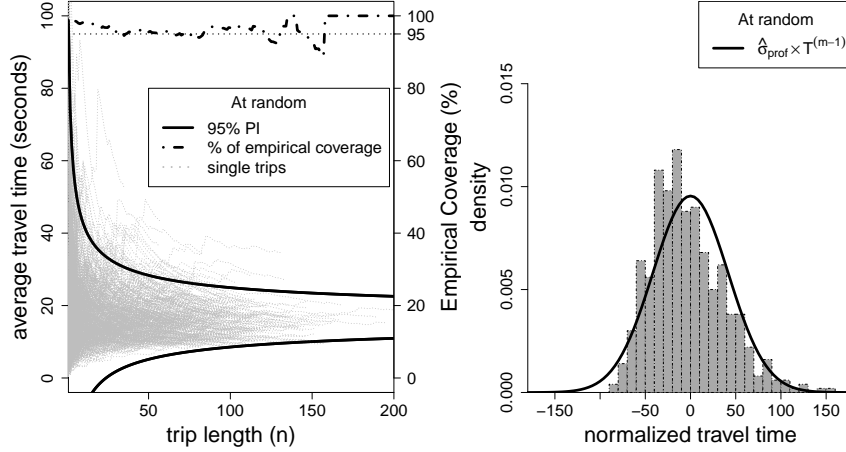


Figure 4: Average $(n^{-1}\mathcal{T}_\rho)$ and normalized $(n + nm^{-1})^{-1/2}(\mathcal{T}_\rho - n\hat{\mu})$ travel time for 500 test trips, sampled at random, plotted on the left and right panels, respectively. PIs of (18) are in solid. Empirical coverage levels, for each n , are in dotted lines (left panel). Right panel prediction density $\hat{\sigma}_{\text{prof}}T^{(m-1)}$ is in solid line. Prediction parameters are in Table 1.

In addition, MAPE drops from 34.8% for trip's with $n < 40$, to 21.5% for trips with $n > 120$. Meanwhile, the empirical coverage probability sustains the theoretical level. For more numerical results on this relation, refer to Appendix Table 6. In both tables, MAPE is the mean absolute percentage error, with geo for geometric mean as the exponential of $n^{-1} \sum_{j=1}^n \log(|n_j \hat{\mu} - \mathcal{T}_\rho^{(j)}|/\mathcal{T}_\rho^{(j)})$; RMSE is the square root of the mean squared error; MAE is the mean absolute error, and ME is the mean error. For coverage metrics, PI rel. length represent the average of PI length divided by the observed travel time.

5.3 Trip-specific prediction interval

In practice, large amount of data is required to estimate $\hat{\mu}_\rho(\tau^*)$ and $\hat{\sigma}_\rho^2(\tau^*)$ of (22) and (24), respectively. Most edges in QCD have less than a handful of speed observations, if any. Without temporal-binning, or a form of interpolation, most of the parameters $(\{m_e, \sigma_e\}, e \in E)$ are inestimable. As in section 5.1, we group all speed observations according to the three traffic-bins (AM, PM, and Otherwise), and calculate three estimates of the mean and variance $\{\hat{m}_e, \hat{\sigma}_e^2\}$, for each edge e .

Figure 5 (left panel) illustrates the trip-specific 95% prediction interval sequences (PS) in (26) in comparison to the asymptotic prediction interval (PI) in (18), for a given trip of

Table 2: Model assessment under different sampling methods, all metrics are in seconds, if not a percentage.

	At random	Stratified sampling from traffic bins			
		Overall	AM	PM	Otherwise
MAPE (geo)	16.64	17.42	15.57	15.63	14.88
RMSE	379.94	382.10	383.43	384.48	288.10
MAE	285.09	291.34	289.79	267.79	194.26
ME	-17.56	27.29	-47.36	15.70	-6.17
MAPE	26.83	24.47	26.59	26.15	23.38
Empirical cov. (%)	94.20	94.74	97.80	93.60	95.60
PI length	1388.1	1363.2	1760.2	1254.5	1022.3
PI rel. length (%)	140.5	134.2	167.9	136.6	137.1

Table 3: Model assessment for trips with different lengths (sampled at random).

	$n \leq 40$	$40 < n \leq 80$	$80 < n \leq 120$	$n > 120$
MAPE	34.84	26.40	24.77	21.48
Empirical cov. (%)	95.00	95.00	94.60	96.00
PI rel. length (%)	242.63	137.51	110.23	92.21

194 edges starting at 7:09 AM, and traveling for 24.8km over a period of 51 minutes. The latter is using the profile estimator $\hat{\sigma}_{\text{prof}}$ of the AM strata, which corresponds to the trip’s bin. As expected, trip-specific PS lead to shorter intervals, for the same level of significance, in comparison to the PI (in sold). All parameter estimates are calculated from a training set sampled from the AM strata, with more details in Appendix F.

With 851 test trips in the AM strata, we calculate the normalized estimated travel time as $\hat{\sigma}_{\rho}^{-1}(\tau^*)(\mathcal{T}_{\rho} - \hat{\mu}_{\rho}(\tau^*))$, for each trip, and plot their histogram in Figure 5 (right panel). In solid blue is the $N(0, 1)$ density, and in solid black the $N(0, \hat{\nu})$ density, where $\hat{\nu}$ as in (25). 95% PIs, based on the former two densities, are in dashed vertical lines in accord with the color code, with 95% empirical coverage intervals (CI) in gray. As expected, the distributional fit of the trip-specific PS are superior to the pool-based PI (Fig. 4),

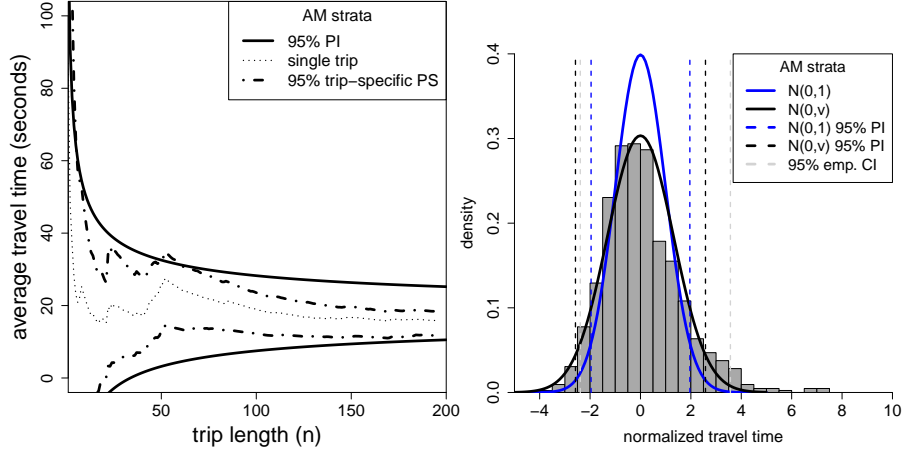


Figure 5: Trip-specific PS of a trip’s average travel time $n^{-1}\mathcal{T}_\rho$ (left) in comparison to the asymptotic prediction interval (PI, in solid) of (18). Histogram of normalized test trips (right) (as $\hat{\sigma}_\rho^{-1}(\tau^*)(\mathcal{T}_\rho - \hat{\mu}_\rho(\tau^*))$) of the AM strata, with a $N(0, 1)$ density depicted in solid blue, $N(0, \hat{\nu})$ in solid black; 95% PI, of the former densities, are in vertical dashed lines in accord with color code; in vertical dashed gray is 95% empirical coverage intervals (CI).

Table 4 reports additional numerical results on a test set of 2000 trips (851 AM strata, 741 PM, and 408 Otherwise). The estimate $\hat{\xi}_G$ is consistently close to 0.3 across all sampling methods (with PM at 0.31, and at random 0.32). This is not surprising, since the average of $\hat{\xi}_G$ across all trips in the training set is 0.3 (see Appendix Figure 6). $\hat{\nu}$ estimates range between 1.31 (AM strata) to 1.45 (sampled at random), with 1.38 for PM, 1.30 for Otherwise and 1.42 for Overall stratas. The integration of $\hat{\nu}$, as a correction scalar to the variance in (26), improves the empirical coverage probability of the trip-specific PS by 10 percentage points. For example, with a random sampling, the empirical coverage went from 84.5% to 94.6%. Under such trip-specific method, the relative length of the PI to the trip’s travel time has dropped significantly from the results of Table 2. For sampling at random, the relative PI length is 81.3%, almost half the asymptotic method of 140.5%. This reduction ratio is consistent for different sampling methods. Other metrics also improved. For example, the mean error dropped from -17.56 to -1.85 seconds, for sampling at random.

Table 4: Model assessment under different sampling methods. Numerical results associated with prediction intervals are listed for $N(0, \hat{\nu})$ and $N(0, 1)$, separated by a comma, all metrics are in seconds, if not a percentage.

	At random	Stratified sampling from traffic bins			
		Overall	AM	PM	Otherwise
MAPE (geo)	8.89	8.89	9.35	9.16	7.57
RMSE	242.17	242.19	259.58	244.74	195.28
MAE	167.60	167.60	185.83	171.26	122.89
ME	-1.85	-1.85	8.13	2.67	-30.91
MAPE	14.403	14.40	15.01	14.65	12.66
Empirical cov. (%)	94.6, 84.5	94.0, 84.2	91.8, 82.7	94.7, 84.8	92.7, 86.5
PI length	850.6, 587.3	827.2, 58.2	810.6, 616.4	855.8, 618.3	631.2, 454.4
PI rel. length (%)	81.3, 56.1	79.1, 55.8	71.4, 54.3	83.0, 60.0	71.7, 51.6

5.4 Comparison to alternative models

We compare our proposed trip-specific PS to that of [Woodard et al. \(2017\)](#)⁶, where they used a Hidden Markov chain model(HMM) to estimate travel time, with edge-specific states representing congestion, which we refer to as HMM. They accounted for other sources of dependency by augmenting the HMM with a trip-specific random effect, which we refer to by TRIP. We also implement a no-dependence (no-dep) model, which assumes no within-trip dependency and no random effect. Prediction intervals for TRIP, HMM and no-dep models, are in accordance with ([Woodard et al., 2017](#), Algo. 2). In particular, for each new trip, we sample 1,000 travel times for the first edge at the start-time traffic bin, and iteratively, for each of 1,000 samples, we sample a travel time of the second edge at the traffic bin of the start-time plus the travel time of the first edge, and so on until the last edge. The predictive intervals are then the empirical intervals of those 1,000 samples of total travel time, and the prediction is the arithmetic mean of those samples.

We also compare our proposed intervals to a regression-based approach that models trip’s travel time, as proposed by [Budge et al. \(2010\)](#); [Westgate et al. \(2013\)](#). In our case, we use a standard linear regression model with the log of travel time as a response variable and total route distance and the time bin of the trip’s start time (categorical) as predictors. The assumptions of the linear regression model hold approximately in QCD.

To estimate parameters, we sample at random 2,000 trips as a test set from QCD, and define the remaining 17,967 trips as a training set. For the trip-specific PS, we estimate edge means and variances for the three traffic-bins using the training set. Values of $\hat{\xi}_G$ of (23)

⁶R-package available at [melmasri.github.io/traveltimeHMM/](https://github.com/melmasri/traveltimeHMM/)

and $\hat{\nu}$ of (25) are estimated to be 0.32 and 1.43, respectively, from a 1,000 randomly selected trips from the training set. The results of the trip-specific PS for the 2,000 test-trips are illustrated in Table 5. Parameters for the prediction intervals proposed by Woodard et al. (2017, Algo. 2) (TRIP, HMM and no-dep) are estimated from the same training set.

Table 5: Comparing trip-specific PS to alternative models; results with $\hat{\nu} = 1$ are in parentheses.

	Trip-specific PS	TRIP	HMM	no-dep	LM
MAPE (geo)	8.82	11.58	11.88	9.96	15.71
RMSE	238.98	366.50	455.08	288.83	368.85
MAE	167.59	220.63	234.00	191.64	271.25
ME	-0.66	-55.24	-92.09	38.04	22.86
MAPE	14.49	18.88	20.02	15.89	24.32
Empirical cov. (%)	94.75 (84.40)	89.40	82.15	73.55	96.60
PI length	855.72 (596.93)	888.93	836.19	520.92	1572.63
PI rel. length (%)	80.56 (56.19)	75.90	70.02	48.53	138.02

Even though TRIP and HMM improved the coverage probability in comparison to the no-dep model, they also reduce the prediction accuracy. MAPE for TRIP is 18.88%, it is 15.89% for the no-dep model. This pattern is consistent with the results of Woodard et al. (2017, Table 1). Our proposed trip-specific PS, improves the prediction accuracy and also achieves the 95% coverage level at tighter PI length (855 seconds) in comparison to TRIP (888 seconds). Our method also achieves negligible bias, -0.66 seconds of mean error.

6 Discussion

Recent work on travel-time estimation focused on empirical approaches Budge et al. (2010); Wang et al. (2019); Westgate et al. (2013); Woodard et al. (2017). We propose a statistical framework for travel-time data on real-world transportation networks. We establish the normality of the ratio of travel time to distance, enabling simple inference methods for travel time and asymptotic prediction intervals. In addition, we propose a predictive distribution that provide trip-specific intervals that are tighter in the short-term than the prediction intervals. Compared to existing methods, we also show that we improve prediction accuracy while obtaining superior coverage levels for smaller prediction intervals. Moreover, the results of Section 3 suggest that the empirical log-normality of travel time is an artifact of the topology of the network, i.e. the distribution of distance defined in urban planning. By conditioning on distance, travel time is at most a mixture of normals.

More generally, our work provides a limit theorem for a type of mixing processes on ergodic dynamical networks. The latter property allows for efficient inference and predictive

methods. Remaining questions exist however and here are a few. Given a distribution of distance, how can the limit distributions be used to simultaneously sample routes and travel time to retrieve back network dynamics mimicking that of the initial input? How to pool route variances to construct an efficient test statistics for difference of percolation regimes, i.e. travel times?

We defined the transportation network G as a directed connected graph, where each edge represents a unique traversable edge segment. Empirically, G is constructed from a physical edge network. To account for topological causal factors affecting the speed distribution, one possible approach is to consider an edge to be a unique traversable segment that has constant features along the whole segment, and hence the endpoints of edges define the node set of G . Regardless of the constructing, our results only depend on n , the number of traveled edges. In this sense, they are invariant to the construction method of G . The construction method only affect the interpretation of the universal parameters (μ, σ) . For example, if the edges of G represent unique 100-meter segments, then μ would represent the average travel time for an arbitrary 100-meter segment. The construction could be trip-specific as well, for example, $\mathcal{T}_\rho / \lfloor |\rho|/100 \rfloor$, where $|x|$ is the length of x in meters, and $\lfloor x \rfloor$ is the largest integer smaller than x .

Speed is known to have few empirical properties that have been shown in various studies. Most importantly, the heavy skewness towards lower speeds, which is discussed extensively by Ma et al. (2017); van Lint et al. (2008), Jenelius and Koutsopoulos (2013, Fig. 8), Woodard et al. (2017, Fig. 3 & 4), and others. Skewness affects the convergence rate to limiting distribution. Such skewness is evident in the right tails of figures 3, 4 and 5, as opposed to the left tail. How large n should be for asymptotics to kick-in? Without an analytical distribution for speed, a theoretical answer is challenging, but an empirical one is possible.

Governments are investing to make transportation-data publicly accessible (the Canadian Open Government initiative⁷ is an example). With such data becoming ubiquitous, deploying our results as part of a practical application provides directions for future work. For example, popular open source projects, such as The OpenStreetMap Project,⁸ provide some road features, but the available information is generally sparse and noisy, since it is updated on voluntary bases. Using traffic-binning from seasonal traffic patterns, as we do for Quebec-City Data (Section 5) and is done in Woodard et al. (2017), it is possible to calculate and store edge specific mean and variance per traffic-bin. Such information can be loaded, and updated, regularly in mobile applications to provide trip-specific PS (Section 4), for arbitrary vehicles and routes. The correlation parameter $\hat{\xi}_G$ of (23) and the residual sample variance $\hat{\nu}$ of (25) can be estimated from a locally stored GPS data. Another ex-

⁷open.canada.ca/en/open-data

⁸www.openstreetmap.org

ample concerns individual vehicles that take routine daily routes (e.g. to work and back). By conditioning on vehicle history, it is possible to use our proposed tools to calculate vehicle(driver)-specific mean and variance parameters to apply the prediction intervals of Equation 18. This enables mobile applications to swiftly calculate trip-specific prediction intervals for vehicles with routine routes from locally stored GPS data, without Internet access and with negligible memory allocation.

References

- Aldous, D. (1991). *Applications of Random Walks on Finite Graphs*, Volume 18 of *Lecture Notes-Monograph Series*, pp. 12–26. Hayward, CA: Institute of Mathematical Statistics.
- Barrat, A., M. Barthelemy, and A. Vespignani (2008). *Dynamical processes on complex networks*. Cambridge university press.
- Benjamini, I. and O. Schramm (2011). Recurrence of distributional limits of finite planar graphs. In *Selected Works of Oded Schramm*, pp. 533–545. Springer.
- Berbee, H. (1987). Convergence rates in the strong law for bounded mixing sequences. *Probability theory and related fields* 74(2), 255–270.
- Billingsley, P. (1965). *Ergodic theory and information*, Volume 1. Wiley New York.
- Bradley, R. C. (2005). Basic properties of strong mixing conditions. a survey and some open questions. *Probab. Surveys* 2, 107–144.
- Britton, T. and P. D. O’Neill (2002). Bayesian inference for stochastic epidemics in populations with random social structure. *Scandinavian Journal of Statistics* 29(3), 375–390.
- Bryc, W. and W. Smoleński (1993). Moment conditions for almost sure convergence of weakly correlated random variables. *Proceedings of the American Mathematical Society* 119(2), 629–635.
- Budge, S., A. Ingolfsson, and D. Zerom (2010). Empirical analysis of ambulance travel times: the case of calgary emergency medical services. *Management Science* 56(4), 716–723.
- Burk, W. J., C. E. Steglich, and T. A. Snijders (2007). Beyond dyadic interdependence: Actor-oriented models for co-evolving social networks and individual behaviors. *International journal of behavioral development* 31(4), 397–404.
- Doyle, P. G. and J. L. Snell (1984). *Random walks and electric networks*, Volume 22. American Mathematical Soc.
- Einsiedler, M. and T. Ward (2013). *Ergodic theory*. Springer.
- Gao, X., H. Xu, and D. Ye (2009). Asymptotic behavior of tail density for sum of correlated lognormal variables. *International Journal of Mathematics and Mathematical Sciences* 2009.

- Geisser, S. (2017). *Predictive inference*. Routledge.
- Getoor, L., N. Friedman, D. Koller, and B. Taskar (2001). Learning probabilistic models of relational structure. In *ICML*, Volume 1, pp. 170–177.
- Ghosh, J., R. Ramamoorthi, and Springer-Verlag (2003). *Bayesian Nonparametrics*. Springer Series in Statistics. Springer.
- Golightly, A. and D. J. Wilkinson (2005). Bayesian inference for stochastic kinetic models using a diffusion approximation. *Biometrics* 61(3), 781–788.
- Guo, F., Q. Li, and H. Rakha (2012). Multistate travel time reliability models with skewed component distributions. *Transportation Research Record: Journal of the Transportation Research Board* (2315), 47–53.
- Herrndorf, N. (1983). The invariance principle for ϕ -mixing sequences. *Zeitschrift für Wahrscheinlichkeitstheorie und Verwandte Gebiete* 63(1), 97–108.
- Hunter, T., T. Das, M. Zaharia, P. Abbeel, and A. M. Bayen (2013). Large-scale estimation in cyberphysical systems using streaming data: a case study with arterial traffic estimation. *IEEE Transactions on Automation Science and Engineering* 10(4), 884–898.
- Hunter, T., R. Herring, P. Abbeel, and A. Bayen (2009). Path and travel time inference from GPS probe vehicle data. *NIPS Analyzing Networks and Learning with Graphs* 12(1), 1–8.
- Jenelius, E. and H. N. Koutsopoulos (2013). Travel time estimation for urban road networks using low frequency probe vehicle data. *Transportation Research Part B: Methodological* 53, 64–81.
- Kallenberg, O. (2006). *Foundations of modern probability*. Springer Science & Business Media.
- Keeling, M. J. and K. T. Eames (2005). Networks and epidemic models. *Journal of the Royal Society Interface* 2(4), 295–307.
- Kolaczyk, E. D. (2009). Models for network graphs. In *Statistical Analysis of Network Data*, pp. 1–44. Springer.
- Kolaczyk, E. D. and G. Csárdi (2014). *Statistical analysis of network data with R*, Volume 65. Springer.
- Limic, V., N. Limić, et al. (2018). Equidistribution, uniform distribution: a probabilist’s perspective. *Probability Surveys* 15, 131–155.
- Lo, C.-F. (2012). The sum and difference of two lognormal random variables. *Journal of Applied Mathematics* 2012.
- Ma, Z., H. N. Koutsopoulos, L. Ferreira, and M. Mesbah (2017). Estimation of trip travel time distribution using a generalized markov chain approach. *Transportation Research Part C: Emerging Technologies* 74, 1–21.

- Nestoridis, V., S. Schmutzhard, and V. Stefanopoulos (2011). Universal series induced by approximate identities and some relevant applications. *Journal of approximation theory* 163(12), 1783–1797.
- Newson, P. and J. Krumm (2009). Hidden markov map matching through noise and sparseness. In *Proceedings of the 17th ACM SIGSPATIAL international conference on advances in geographic information systems*, pp. 336–343. ACM.
- Norets, A. (2010). Approximation of conditional densities by smooth mixtures of regressions. *The Annals of statistics* 38(3), 1733–1766.
- Oppenlander, J. C. (1976). Sample size determination for travel time and delay studies. *Traffic Engineering* 46(9).
- Peligard, M. and R. Suresh (1995). Estimation of variance of partial sums of an associated sequence of random variables. *Stochastic processes and their applications* 56(2), 307–319.
- Peligrad, M. (1996). On the asymptotic normality of sequences of weak dependent random variables. *Journal of Theoretical Probability* 9(3), 703–715.
- Ramsay, J. O., G. Hooker, D. Campbell, and J. Cao (2007). Parameter estimation for differential equations: a generalized smoothing approach. *Journal of the Royal Statistical Society: Series B (Statistical Methodology)* 69(5), 741–796.
- Rosenblatt, M. (1956). A central limit theorem and a strong mixing condition. *Proceedings of the National Academy of Sciences of the United States of America* 42(1), 43.
- Salazar, M., F. Rossi, M. Schiffer, C. H. Onder, and M. Pavone (2018, Nov). On the interaction between autonomous mobility-on-demand and public transportation systems. In *2018 21st International Conference on Intelligent Transportation Systems (ITSC)*, pp. 2262–2269.
- Snijders, T., C. Steglich, and M. Schweinberger (2017). Modeling the coevolution of networks and behavior. In *Longitudinal models in the behavioral and related sciences*, pp. 41–71. Routledge.
- van Lint, J., H. J. van Zuylen, and H. Tu (2008). Travel time unreliability on freeways: Why measures based on variance tell only half the story. *Transportation Research Part A: Policy and Practice* 42(1), 258–277.
- Volkonskii, V. and Y. A. Rozanov (1959). Some limit theorems for random functions. i. *Theory of Probability & Its Applications* 4(2), 178–197.
- Wang, H., X. Tang, Y.-H. Kuo, D. Kifer, and Z. Li (2019). A simple baseline for travel time estimation using large-scale trip data. *ACM Transactions on Intelligent Systems and Technology (TIST)* 10(2), 19.

- Westgate, B. S., D. B. Woodard, D. S. Matteson, S. G. Henderson, et al. (2013). Travel time estimation for ambulances using bayesian data augmentation. *The Annals of Applied Statistics* 7(2), 1139–1161.
- Weyl, H. (1916). Über die gleichverteilung von zahlen mod. eins. *Mathematische Annalen* 77(3), 313–352.
- Woodard, D., G. Nogin, P. Koch, D. Racz, M. Goldszmidt, and E. Horvitz (2017). Predicting travel time reliability using mobile phone GPS data. *Transportation Research Part C: Emerging Technologies* 75, 30–44.
- Wu, W. B. (2009). Recursive estimation of time-average variance constants. *The Annals of Applied Probability* 19(4), 1529–1552.
- Zheng, F. and H. J van Zuylen (2013). Urban link travel time estimation based on sparse probe vehicle data. *Transportation Research Part C: Emerging Technologies* 31, 145–157.

Appendices

A Proof of Lemma 3.1

Proof. For every trip, the almost sure convergence follows directly from the fact that speed is bounded on each edge and by applying Theorem 2.2 of [Bryc and Smoleński \(1993\)](#) stated in the following lemma. Suppose $(X_i, i \in \mathbb{Z})$ are a sequence of real random variables defined on a probability space (Ω, \mathcal{F}, P) . For some $A \subset \mathbb{Z}$, define the σ -field $\mathcal{F}_A = \sigma(X_i, i \in A)$. For $n \geq 0$, let

$$\tilde{r}(n) = \sup \left| \text{Corr} \left(\sum_{a \in A} X_a, \sum_{b \in B} X_b \right) \right|, \quad (27)$$

where the supremum is taken over all finite subset $A, B \subset \mathbb{Z}$ that are n distance apart, $\text{dist}(A, B) \geq n$.

Lemma A.1 (Thm 2.2 in [Bryc and Smoleński \(1993\)](#)). *If $\tilde{r}(k) < 1$ for some $k > 0$, $\mathbb{E}[X_k] = 0$ for all k , and*

$$\sum_{k=1}^{\infty} k^{-3/2} \mathbb{E}[X_k^2] < \infty, \quad (28)$$

then $n^{-1} \sum_{k=1}^n X_k \rightarrow 0$ almost surely.

Clearly $\tilde{r}(k) \leq \rho^*(k)$ of Definition 2.2. By Assumption 1 and Definition 2.3, we have $\mathbb{E}[(d_e S_e)^2] < C$ for some constant $C < \infty$, satisfying (28). By Birkhoff’s point-wise ergodic theorem, [Billingsley \(1965, Thm 1.3\)](#), Lemma C.4 Appendix C, without extra conditions on the system, $n^{-1} \mathcal{T}_\rho$ converges to a constant μ that depends on initial conditions t_0 , and route ρ . \square

B Proof of Theorems 3.2 and 3.4

Proof of Theorem 3.2 and 3.4 follow directly from (Peligrad, 1996, Thm 2.2 & Coro. 2.2). Following Bradley (2005), and Definition 2.2, let $\{X_{ni}, 1 \leq i \leq k_n\}$ and $n \in \mathbb{Z}$ be a triangular array of the random variables $(X_i, i \in \mathbb{Z})$, where $k_n \rightarrow \infty$. Let ρ^*_{max} be a dependency measure between any two non-empty subsets $A, B \subset \{1, 2, \dots, k_n\}$ of rows of the array that are at least k distance apart, as

$$\rho^*_{max}(k) := \sup_k |\rho^*(\sigma(X_{ni}, i \in A), \sigma(X_{ni}, i \in B))|, \quad \text{dist}(A, B) \geq k. \quad (29)$$

Lemma B.1 (Thm 2.2 & Coro. 2.2 Peligrad (1996)). *Let $(X_i, i \in \mathbb{Z})$ be a strongly mixing sequence, with $\mathbb{E}[X_i] = 0$ for all i and $\inf_i \mathbb{E}[X_i^2] > 0$, where $(X_i^2, i \in \mathbb{Z})$ is a uniformly integrable family. Define the triangular array $\{a_{ni}X_i, 1 \leq i \leq n\}$, for some constants $\{a_{ni}\}$, and denote $\sigma_n^2 = \mathbb{E}[(\sum_{i=1}^n a_{ni}X_i)^2]$. Assume that*

$$\max_{1 \leq i \leq n} \frac{|a_{ni}|}{\sigma_n} \rightarrow 0, \quad \text{as } n \rightarrow \infty, \quad (30)$$

if $\rho^*_{max}(1) < 1$ then $\sigma_n^{-1} \sum_{i=1}^n a_{ni}X_i \xrightarrow{d} N(0, 1)$.

Proof of Theorem 3.2. By Lemma 3.1, we know that $n^{-1}\mathcal{T}_\rho \xrightarrow{a.s.} \mu(t_o, \rho)$. Without loss of generality, assume \mathcal{T}_ρ is centered. Condition (30) follows directly from the definition a transportation network, where $(d_e, e \in E)$ are bounded and $\sigma_\rho \rightarrow \infty$. By Assumption 1, we have $\inf_e \mathbb{E}[S_e^2] > 0$, and since $(S_e, e \in E)$ are uniformly bounded, then they are uniformly integrable. $\rho^*_{max}(1) < 1$ follows from the condition that $\rho^*(1) < 1$ in definition 2.3. \square

Proof of Theorem 3.4 Follows directly from the proof of 3.2 above, while Theorem 3.3 insures that $n^{-1}\mathcal{T}_\rho \xrightarrow{a.s.} \mu$.

C Proof of Theorem 3.3

Proof of Lemma 3.3 builds on the literature of dynamical systems and Birkhoff's Ergodic Theorem. The proof is illustrated with a series of definitions and lemmas. We use (X, \mathcal{B}, μ) to refer to a probability space associated with a random variable X having a σ -finite Borel algebra \mathcal{B} and a probability measure μ , such that $\mu(X) = 1$.

Definition C.1. *A measure-preserving system (or a dynamical system) is the quadruple (X, \mathcal{B}, μ, T) , where (X, \mathcal{B}, μ) is a probability space, and $T : X \rightarrow X$ is a measure-preserving map such $T^{-1}A \in \mathcal{B}$ and $\mu(T^{-1}A) = \mu(A)$ for all $A \in \mathcal{B}$; that is T is μ -measurable and μ -invariant.*

T^{-1} is the inverse of T . A series of measure-preserving transformations define an orbit around a initial point $x_o \in X$, as

$$\{x_0, Tx_o, T^2x_o, \dots, T^n x_o := T \circ T \circ \dots \circ Tx_o\}.$$

Definition C.2. Let (X, \mathcal{B}, μ, T) be a measure-preserving system, and let $A \in \mathcal{B}$. We say the orbit $(T^n x_0)_{n \geq 0}$ equidistributes in A if

$$\lim_{N \rightarrow \infty} \frac{1}{N} \# \{n \in \{0, 1, \dots, N-1\} : T^n x_0 \in A\} \rightarrow \mu(A) \text{ a.s.}$$

Further, we say T is **equidistributing**, if for every $A \in \mathcal{B}$ the orbit $(T^n x_0)_{n \geq 0}$ equidistributes in A for almost every $x_0 \in X$.

In a sense, the frequency distribution of the number of visits to A converges to $\mu(A)$ almost surely.

Definition C.3. A measure-preserving system (X, \mathcal{B}, μ, T) is called **ergodic**, if for any $A \in \mathcal{B}$ such that $T^{-1}A = A$, implies that $\mu(A) = 0$ or $\mu(A) = 1$.

Lemma C.4 (Thm 1.3 Billingsley (1965)). On a probability space (X, \mathcal{B}, μ) , let $T : X \rightarrow X$ be a measure-preserving transformation, if a function f is $L^1(X, \mathcal{B}, \mu)$, then there exists a $L^1(X, \mathcal{B}, \mu)$, invariant function, g such that $\int g d\mu = \int f d\mu$, and

$$\lim_{n \rightarrow \infty} \frac{1}{n} \sum_{k=0}^{n-1} f(T^k x_0) = g(x_0) \quad \text{a.e (almost everywhere)} \quad (31)$$

If the system is ergodic, i.e. T is equidistributing, then $g(x_0) = \int f d\mu$ a.e.

Essentially, ergodicity entails that the system tends to forget the initial value x_0 . Lemma C.4 is an adaptation of (Billingsley, 1965, Thm 1.3), thus will not be proven. To prove our results, we need the following lemma and example.

Example C.5 (Prop. 2.16 Einsiedler and Ward (2013)). Let $([0, 1], \mathcal{B}([0, 1]), \lambda)$ be the $[0, 1]$ metric space equipped with the Lebesgue measure λ . Let $Tx = T(x) \pmod{1} := x + \alpha \pmod{1}$, then if $\alpha \in \mathbb{R} \setminus \mathbb{Q}$ (irrationals) the system is ergodic, if $\alpha \in \mathbb{Q}$, the system is not ergodic.

Example C.5 will be used in our proof, however we require a probabilistic version of it, which can be deduced by the recent results of Limic et al. (2018). We define a probabilistic mapping $T_k : [0, 1] \mapsto [0, 1]$ to be a rotation of Example C.5 indexed by i.i.d uniform random numbers, such that $T_k x = T_k(x) \pmod{1} = x + u_k \pmod{1}$, where $u_k \stackrel{i.i.d}{\sim} \text{Uniform}[0, 1]$. The measure-preserving system $([0, 1], \mathcal{B}([0, 1]), \lambda, (T_k)_k)$, is a random system; random in the sense that T_k is a random mapping functions. A general family of maps (not necessary random) $\mathbf{T} : [0, 1] \mapsto [0, 1]$ is sufficiently mixing to be equidistributing, if, and only if, the Weyl criterion (Weyl, 1916) $W_N(\mathbf{T}, m)$ goes to 0 (λ -a.s) as $N \rightarrow \infty$, where

$$W_N(\mathbf{T}, m) := \frac{1}{N} \sum_{k=1}^N \exp(2\pi i m T_k), \quad (32)$$

for all $m \in \mathbb{Z} \setminus \{0\}$. The above characterization comes from Fourier analysis. In dimension 1, the class of complex exponentials $x \mapsto \exp(2\pi i m x)$, $m \in \mathbb{Z}$ is orthonormal in $L^2[0, 1]$, and by the

Stone-Weierstrass theorem, such class is dense in the periodic continuous functions on $[0, 1]$ with respect to the sup-norm. [Limic et al. \(2018\)](#) defined a Wely-like probabilistic criterion by defining the following random variable

$$Y_k(m) := \exp(2\pi im T_k), \quad (33)$$

for random maps $\mathbf{T} = (T_k)_k, T_k : [0, 1] \mapsto [0, 1]$.

Lemma C.6 (Sufficiency for complete equidistribution, Lem 2.2 of [Limic et al. \(2018\)](#)). *Let $(T_k)_k$ be a sequence of random maps, and $Y_k(m)$ be as in (33). If for each $m \in \mathbb{Z} \setminus \{0\}$*

$$|\mathbb{E}Y_k(m)\bar{Y}_l(m) + Y_l(m)\bar{Y}_k(m)| = O(|k - l|^\delta), \quad (34)$$

for some $\delta(m) > 0$, then $(T_k)_k$ is completely equidistributed in $[0, 1]$.

The following Corollary is a direct result for Lemma C.6.

Lemma C.7. *Let $([0, 1], \mathcal{B}([0, 1]), \lambda)$ be the $[0, 1]$ metric space equipped with the Lebesgue measure λ . Let $T_k x = T_k(x) \pmod{1} = x + u_k \pmod{1}$, for $u_k \stackrel{i.i.d.}{\sim} \text{Uniform}[0, 1]$, then, $([0, 1], \mathcal{B}([0, 1]), \lambda, (T_k)_k)$ is ergodic.*

Proof. By Lemma C.4 and Example C.5, we know that the system is measure-preserving, to show that it is ergodic, it suffices to satisfy condition (34) of Lemma C.6. Note that for any $x \in [0, 1]$, $T_1(x) = x + u_1$, and $T_k(x) = T_1 \circ T_2 \cdots \circ T_k(x) = x + \sum_{i=1}^k u_i$. For each $m \in \mathbb{Z} \setminus \{0\}$, let $s = \sum_{i=l}^k u_i$, then

$$\mathbb{E}[Y_k \bar{Y}_l + Y_l \bar{Y}_k](m, x) = \mathbb{E} \left[\exp(2\pi im \sum_{i=l}^k u_i) + \exp(-2\pi im \sum_{i=l}^k u_i) \right] \quad (35)$$

$$= 2 \int_{[0, 1]^{|k-l|}} \cos(2\pi ms) ds \quad (36)$$

$$= 0 \quad (37)$$

□

Proof of Theorem 3.3. Our first condition is that ρ is a random walk on G . Without loss of generality, we will assume that every edge e has unit length (i.e. $(d_e = 1, e \in E)$), thus, travel time becomes

$$\mathcal{T}_\rho = \sum_{e \in \rho} m_e(\tau) + \sum_{e \in \rho} \epsilon_e(\tau).$$

By construction $(\epsilon_e(\tau), e \in \rho)$ is α -mixing, further, by Definition 2.3, Lemma 3.1 and its proof in Appendix A, we have $n^{-1} \sum_{e \in \rho} \epsilon_e(\tau) \xrightarrow{a.s.} 0$. It remains to show that $n^{-1} \sum_{e \in \rho} m_e(\tau)$ converges to a constant that is independent from initial conditions.

By Definition 2.3 we know that G has a finite node set N , we denote it by G_N . By construction, transportation networks have bounded degrees $\sup_{e \in E} \deg(e) < C_1$ for some $C_1 < \infty$. From Polya's Theorem on recurrence in the plane, see [Doyle and Snell \(1984, Sec. 2.14\)](#) and [Benjamini and](#)

Schramm (2011, Thm. 1.1, Cor. 1.2), G is recurrent with probability 1 (G_N is a 2-dimensional planar graph).

Our transportation network G is equipped with random bounded weights $(S_e, e \in E)$. Since G is finite, and $(S_e, e \in E)$ are bounded away from 0, then the transportation network is also recurrent with probability 1.

For each $e \in E$, let $(\tau_i(e))_i$ be the the almost sure recurrent random times of e . By the recurrence property we have $\tau_i(e) < \infty$ a.s. for all $i \in \mathbb{Z}$. Define $Z_i(e) = \tau_i(e) - \tau_{i-1}(e)$ for $i > 1$, and $Z_1(e) := \tau_1(e) - t_0$, the recurrence time difference. By stationarity of G , $(Z_i(e))_i$ are independent stationary random variables.

We first treat each edge $e \in E$ separately, and show that

$$\frac{1}{n_e} \sum_{i=1}^{n_e} m_e(\tau_i) \rightarrow \mu_e,$$

where μ_e is a constant that is independent of recurrence times $(\tau_i(e))_i$, and n_e is the count of the latter.

By continuity of $m_e(t)$, it is Lebesgue measurable (λ -measurable). Let a be the length of the seasonality cycle of $m_e(t)$. Then m_e is $L^1([0, a], \mathcal{B}[0, a], \lambda)$.

By Example C.5 and Lemma C.7, $(\tau_i(e))_i$ define an equidistributing rotation mapping on the circle $[0, a]$, with initial point $x_0 = t_0 + Z_1(e) \pmod{a}$, such that

$$(\tau_i(e))_i = \left(x_0, T x_0 = x_0 + Z_2(e) \pmod{a}, T^2 x = T x_0 + Z_3(e) \pmod{a}, \dots \right).$$

Then

$$\frac{1}{n_e} \sum_{i=1}^{n_e} m_e(\tau_i) = \frac{1}{n_e} \sum_{i=1}^{n_e} m_e(T^i x_0) \xrightarrow{n_e} \frac{1}{a} \int_0^a m_e(\lambda) d\lambda \quad (a.e.) \quad (38)$$

By Theorem C.4, $\int_0^a m_e(\lambda) d\lambda$ is independent of initial conditions, the $\frac{1}{a}$ is to convert the integral to a probability. It is easy to see that

$$\frac{1}{a} \int_0^a m_e(\lambda) d\lambda = \mathbb{E}[m_e] = \mathbb{E}[\mathbb{E}[S_e(t)]] = \mathbb{E}[S_e] = \mu_e,$$

the unconditional expected speed. the Towers property was used since under stationarity, t is an index of sub- σ -algebras $\mathcal{F}_t \subset \mathcal{F}$, where \mathcal{F} is the space of events of S . This is not surprising since ergodic dynamical systems have the property that space averaging equals time averaging (the sum in (38)). Combining our results,

$$\frac{1}{n} \sum_{e \in \rho} m_e(\tau) = \sum_{e \in E} \frac{n_e}{n} \frac{1}{n_e} \sum_{i=1}^{n_e} m_e(\tau_i) \xrightarrow{n} \sum_{e \in E} \pi_e \mu_e = \mu, \quad a.s. \quad (39)$$

By Empirical process theory we have $n_e/n \xrightarrow{a.s.} \pi_e \in [0, 1]$ a constant such that $\sum_{e \in E} \pi_e = 1$, hence μ is the invariant expected speed over the map G .

If ρ a simple random walk, then π_e would be proportional to the degree distribution of e , otherwise proportional to the weights assigned to e . \square

D Proof of Theorem 4.1

Our proof of Theorem 4.1 builds on the following lemma on central limit theorem for random rotation maps.

Lemma D.1 (CLT for random rotations). *Let $\Xi = \mathbb{R}/\mathbb{Z}$ be the unit circle, equipped with Lebesgue measure λ . Define $T : \Xi \rightarrow \Xi$ to be a random rotation mapping, such that $T^k x = x + u_k$, where $u_k \stackrel{i.i.d.}{\sim} \text{Uniform}[0, 2\pi]$. For a function, $f : \Xi \mapsto \mathbb{R}$, $f \in L^2(\lambda)$ with $\int_{\Xi} f d\lambda = 0$, for any $x \in \Xi$, we have*

$$\frac{1}{\sqrt{n}} \sum_{k=1}^n f(T^k x) \xrightarrow{d} N\left(0, \int f^2 d\lambda\right).$$

Proof. Irrationals are dense in \mathbb{R} , hence an absolutely continuous random variables is almost surely irrational. By Example C.5, T in Lemma D.1 is ergodic. By construction and Kallenberg (2006, Thm. 5.10), for any $x \in \Xi$, the family $(T^k x)_{k \geq 1} \stackrel{d}{=} (U_k)_{k \geq 1}$, where $U_k \stackrel{i.i.d.}{\sim} \text{Uniform}[0, 2\pi]$. Since $f \in L^2(\lambda)$, by Kallenberg (2006, Thm. 5.11), there exist a random variable $X_k \in \mathbb{R}$, such that $X_k \stackrel{a.s.}{=} f(U_k)$ for all k , with $\mathbb{E}X_k = 0$. By classical central limit theorem Kallenberg (2006, Prop. 4.9), we have

$$\frac{1}{\sqrt{n}} \sum_{i=1}^n f(T^i x) \stackrel{d}{=} \frac{1}{\sqrt{n}} \sum_{i=1}^n X_k \xrightarrow{d} N(0, \mathbb{E}X_1^2).$$

□

Proof of Theorem 4.1. With Theorem 3.4, let $n = |\rho|$, we decompose (21) as,

$$\frac{\mathcal{T}_\rho - \mu_\rho(\tau^*)}{\sigma_\rho(\tau^*)} = \frac{\mathcal{T}_\rho - n\mu}{\sigma_\rho(\tau^*)} - \frac{\mu_\rho(\tau^*) - n\mu}{\sigma_\rho(\tau^*)} = I - II. \quad (40)$$

By Theorem 3.4 and Slutsky's theorem we have,

$$I = \frac{\sqrt{n}\sigma}{\sigma_\rho(\tau^*)} \frac{\mathcal{T}_\rho - \mu_\rho(\tau)}{\sqrt{n}\sigma} \xrightarrow{d} \sqrt{\eta}N(0, 1), \quad \eta = \lim_{n \rightarrow \infty} \frac{n\sigma^2}{\sigma_\rho^2(\tau^*)}. \quad (41)$$

For II we will first show that $n^{-1}\mu_\rho(\tau^*) \xrightarrow{a.s.} \mu$. which requires the deterministic times $\tau^* = (\tau^*(e), e \in \rho)$ to be equidistributing. For a route $\rho = \langle e_1, e_e, \dots \rangle$, we can write $n^{-1}\mu_\rho(\tau^*)$ as

$$\frac{1}{n}\mu_\rho(\tau^*) = \frac{1}{n} \sum_{e \in \rho} m_e(\tau^*) = \sum_{e \in E} \frac{n_e}{n} \frac{1}{n_e} \sum_{i=1}^{n_e} m_e(\tau_i^*(e)),$$

where $\tau_i^*(e)$ is the i th entrance time to edge e , for $i = 1, \dots, n_e$. Hence it suffices to show that $n_e^{-1} \sum_{i=1}^{n_e} m_e(\tau_i^*(e)) \xrightarrow{a.s.} \mu_e$. From the proof of Theorem 3.3, and (39) in particular, we have that $n_e/n \xrightarrow{a.s.} \pi_e \in [0, 1]$, and hence $\mu = \sum_{e \in E} \pi_e \mu_e$.

Following the proof arguments of Theorem 3.3 in Appendix C, and the fact the ρ is a random walk on G , from the recurrence property in 2-dimensional planar graphs, we have $\tau_i^*(e) < \infty$ a.s. for all $i \in \mathbb{Z}$.

Without loss of generality, define $U_i(e) = \tau_i^*(e) - \tau_{i-1}^*(e)$ for $i > 1$, the recurrence time difference, with $U_1(e) = \tau_1^*(e) - t_0$, where t_0 is the start time of the trip. By stationarity of G , $(U_i(e))_i$ are independent stationary random variables.

Assume that the period of each $(m_e(t), e \in E)$ is of length $a > 0$. Since $m_e(t) \in L^2(\lambda)$ (λ is the Lebesgue measure), by Example C.5 and Lemma C.7, $(\tau_i^*(e))_i$ define an equidistributing rotation mapping on the circle $[0, a]$, with initial point t_0 , such that $\tau_1^*(e) = Tt_0 = t_0 + U_1(e) \pmod{a}$, for a mapping $T : [0, a] \rightarrow [0, a]$. By similar arguments used in (38) and (39), we have $n^{-1}\mu_\rho(\tau^*) \xrightarrow{a.s.} \mu$.

It remains to show that $n^{-1/2}(\mu_\rho(\tau^*) - n\mu) \xrightarrow{d} N(0, \tilde{\sigma}^2)$, or equivalently

$$\sum_{e \in E} \frac{\sqrt{n_e}}{\sqrt{n}} \frac{1}{\sqrt{n_e}} \sum_{i=1}^{n_e} \left(m_e(\tau_i^*) - \mu_e \right) \xrightarrow{d} N(0, \tilde{\sigma}^2). \quad (42)$$

It suffices to establish that $n_e^{-1/2}(\sum_{i=1}^{n_e} m_e(\tau_i^*) - \mu_e) \xrightarrow{d} N(0, \sigma_e^2)$, for every $e \in E$, where $\sigma_e^2 = \int_{C_e} m_e^2(t) dt - \left(\int_{C_e} m_e(t) dt \right)^2$; which is established by Lemma D.1. Since by Assumption 2, conditional on speed regimes Π , and the propriety of the sum of independent normal variables, (42) holds with

$$\tilde{\sigma}^2 = \sum_{e \in E} \pi_e \sigma_e^2 = \sum_{e \in E} \pi_e \left[\int_{C_e} m_e^2(t) dt - \left(\int_{C_e} m_e(t) dt \right)^2 \right].$$

Finally, by across-trip dependency $I \perp\!\!\!\perp II$, moreover, at the limit, both I and II are independent of Π . \square

E Exploratory analysis of Quebec city data

E.1 Data preparation

Quebec city 2014 GPS data (QCD) is collected using the Mon Trajet smartphone application (developed by Brisk Synergies Inc). This study made use of a sample of open data, which contained over 4000 drivers and 21,872 individual trips. No personal identifiers of drivers were available. The precise duration of the time period is kept confidential. The application was installed voluntarily by drivers who anonymously logged trips using a simple interface.

No measure was provided to insure the validity of trips; i.e., if they are composed solely from motorized vehicles, excluding walkers, bikers, and non-traffic interruptions. The data is processed by breaking down trips into multiple trips whenever i) trips include idle time (a period of no move) of more than 4 minutes; or ii) there is more than 2 minutes between consecutive GPS observations. After decomposition, we trim end-points of trips, such that each trip starts whenever the driving speed is larger than 10km/h for the first time, and ends whenever the driving speed is less than 10km/h for the last time.

To remove non-motorized travel, we remove trips with i) median speed less than 20km/h; ii) maximum speed less than 35km/h, or ii) when driving distance is less than 1km (as measured

by the sum of the great circle distances between pairs of sequential measurements). Those three requirements appear to eliminate most walking and biking travel (Woodard et al., 2017).

We estimate the total travel time per edge by calculating i) within-edge travel time, as the time spent within the edge, and ii) across-edge travel time, as the time spent crossing other edges; the time spent between the closest two GPS observations, where one is in the edge the other in the adjacent edge. In the same way we calculate across-edge distance. The total travel time per edge is then 100% of within-edge plus across-edge travel time weighted by half the proportion of across-edge distance to the total length of the edge. Total edge-lengths are obtained from OSM. We treat intermediate edges, those without GPS observations, as a single edge and calculate the total travel time over it, and then assign it proportionally to the length of each intermediate edge. With these total travel time estimates, we calculate the (reciprocal of) average speed per edge by dividing the total travel time by total length, for fully traveled edges, and by partial lengths otherwise. Partial lengths are the distance covered by the vehicle to the traveled end-point of the edge.

F Traffic-bin estimators

Initial cleaning of the QCD results in 19,967 trips. The data is split in a training set of 17,967 trips and a test set of 2,000 trips, the latter includes 851 trips from the AM strata, 741 from the PM, and 408 otherwise. We require at least a single observation per edge \times time bin category. Therefore, the test set is sampled randomly such that with every new sample introduced to the test set, the test set, when removed from the QCD, does lead to edges \times time bin with no observation. The remaining trips are using as a training set.

The map-version estimators $(\hat{m}_e, \hat{\sigma}_e^2, e \in E)$ are calculated using the training set. For each edge \times time bin, we use the average of all observations to calculate the sample mean \hat{m}_e , and similarly, we use the classical sample variance estimator to calculate $\hat{\sigma}_e^2$. Since all our notations use the path-conditioning ($e \in \rho$), the sample mean and variance are implemented on the edge-graph and not the graph G directly. In particular, for every edge e with k exits $\{e_1, \dots, e_k\}$ we have $k \times \#\{\text{time bins}\}$ estimators for m_e , each represents $\mathbb{E}[S_e(t)|\langle e, e_i \rangle, t \in \text{time bin}]$ and $\mathbb{V}(S_e(t)|\langle e, e_i \rangle, t \in \text{time bin})$ for $i = 1, \dots, k$. For each trip, the notation $(\{\hat{m}_e, \hat{\sigma}_e^2\}, e \in \rho)$ correspond exactly to the path-conditioning estimators. We use the three traffic bins introduced in section 5 to classify the time bins.

We require at least 10 observations per unit $(\{\langle e, e_i \rangle, \text{time bin}\})$ for the estimators $(\hat{m}_e, \hat{\sigma}_e^2, e \in E)$ to be used in practice. Approximately 90% of units have less than 10 observations. We impute those quantities in the following order; a) removing path-conditioning, i.e. impute by the M-estimate of $\mathbb{E}[S_e(t)|t \in \text{time bin}]$ when $\mathbb{E}[S_e(t)|\langle e, e_i \rangle, t \in \text{time bin}]$ is inestimable; and by b) removing edge-conditioning, i.e impute by the M-estimate of $\mathbb{E}[S(t)|t \in \text{time bin}]$ when a) is inestimable. Even though this imputation procedure is crude, the results are promising.

G Additional results

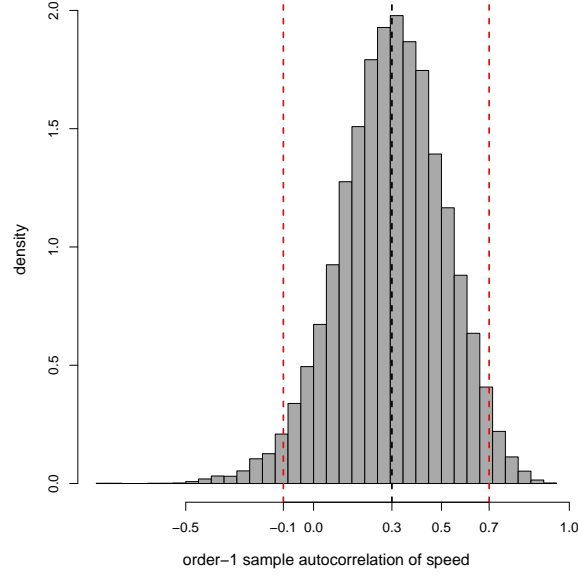


Figure 6: Histogram of ξ_G if (23) of all trips in the training of 17967 trips described in Section 5.4. The mean is indicated with black dashed lines, and the 95% empirical confidence intervals are in dashed red.

Table 6: Model assessment under different sampling methods, all metrics are in seconds, if not a percentage.

	At random	Stratified sampling from traffic bins			
		Overall	AM	PM	Otherwise
MAPE (geo)	16.64	17.42	15.57	15.63	14.88
RMSE	379.94	382.10	383.43	384.48	288.10
MAE	285.09	291.34	289.79	267.79	194.26
ME	-17.56	27.29	-47.36	15.70	-6.17
MAPE	26.83	24.47	26.59	26.15	23.38
Empirical cov. (%)	94.20	94.74	97.80	93.60	95.60
PI length	1388.1	1363.2	1760.2	1254.5	1022.3
PI rel. length (%)	140.5	134.2	167.9	136.6	137.1

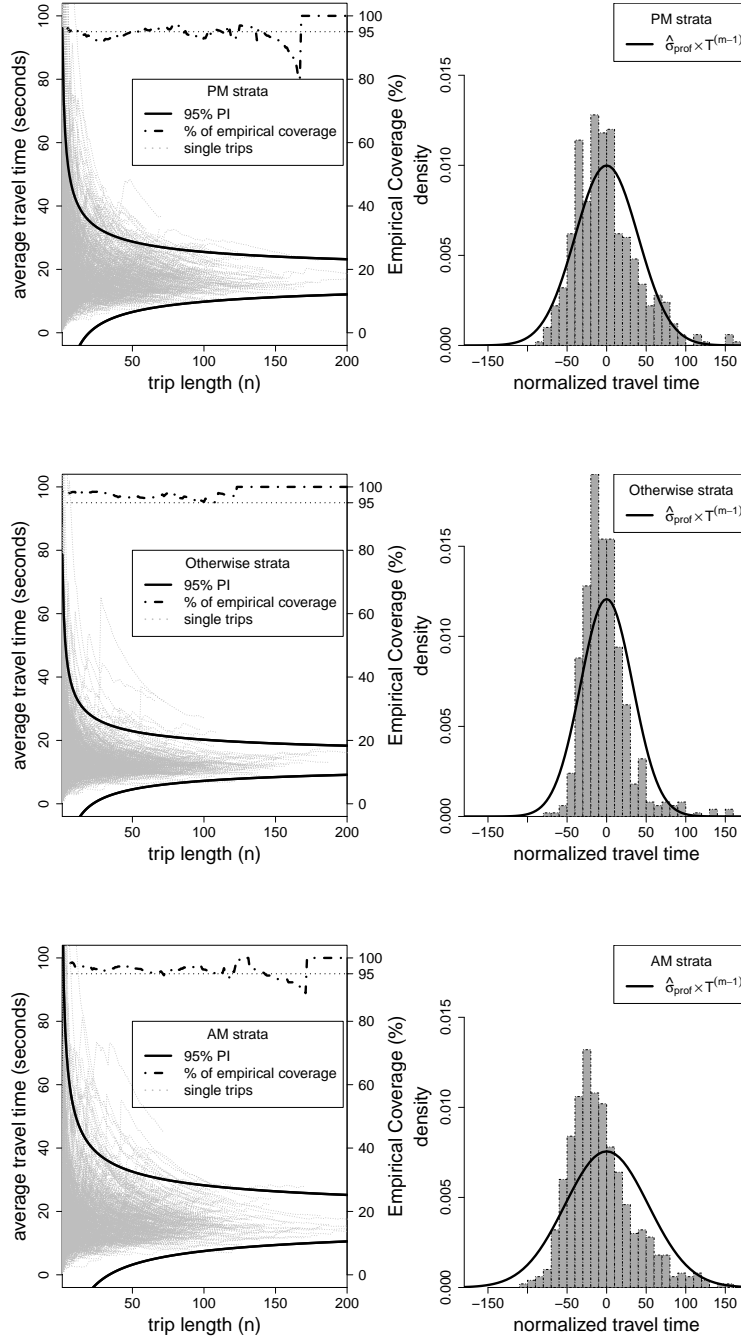


Figure 7: Average $(n^{-1}\mathcal{T}_\rho)$ and normalized $(n + nm^{-1})^{-1/2}(\mathcal{T}_\rho - n\hat{\mu})$ travel time for 500 test trips plotted on the left and right panels, respectively. Tests trips are sampled from PM strata (top row) and from the Otherwise strata (bottom row). Prediction intervals of (18) are in solid lines. Empirical coverage levels, for each n , are in dotted lines (left panel). Right panel prediction density $\hat{\sigma}_{\text{prof}}T^{(m-1)}$ is in solid lines. Prediction parameters are from Table 1 in accordance with the sampling method.

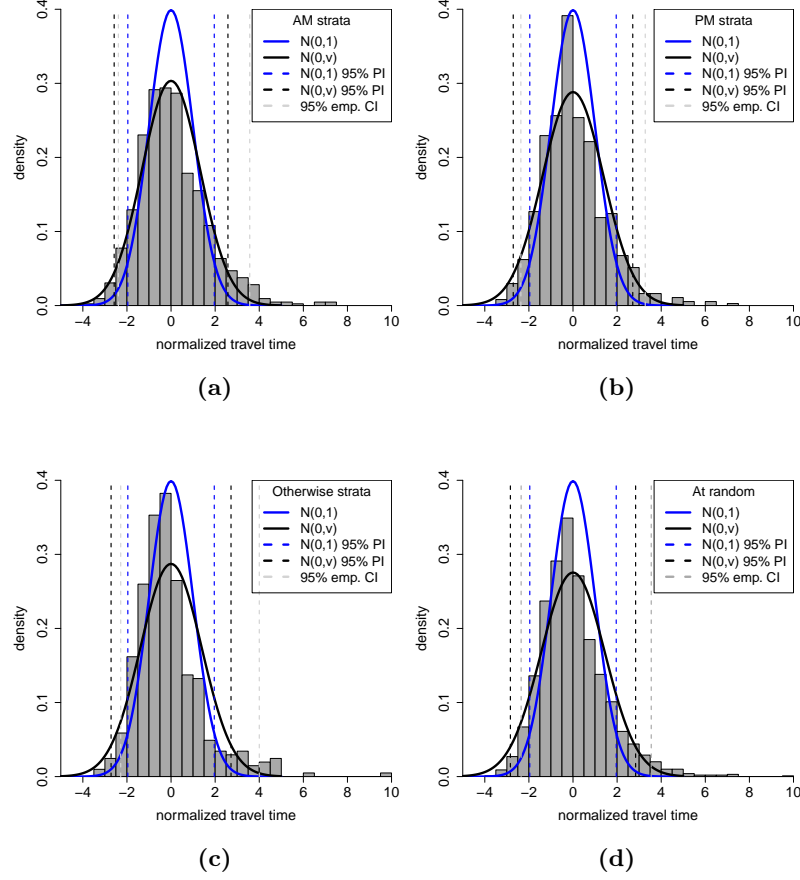


Figure 8: Histogram of normalized trips (as $\hat{\sigma}_\rho^{-1}(\tau^*)(\mathcal{T}_\rho - \hat{\mu}_\rho(\tau^*))$) from the test set under different sampling methods, with a $N(0, 1)$ density depicted in solid black, $N(0, \hat{v})$ in solid blue; 95% prediction intervals are in vertical dashed lines in accordance with color; in vertical dashed gray is the 95% empirical coverage intervals.